University of Trento

Department of Physics

Degree course in Physics

Final Thesis

Resonances in quantum elastic scattering: a time-dependent numerical investigation

Supervisor:

Giovanni Garberoglio

Graduant:

Alberto Bailoni

Academic Year 2013/2014

Contents

List of Figures

List of Tables

Introduction

Resonances are well defined peaks observed in the total cross section of quantum scattering processes as a function of the energy of the system. Unfortunately, experiment cannot provide details on the origin of these features.

In this thesis, we will investigate quantum scattering processes by numerically solving the time-dependent Schrödinger equation, in the specific case of the hydrogen-krypton scattering.
We will discuss how scattering resonances are related to an increase of the probability, observed at some specific energies, of finding the scattered particle close to the interaction center.

In the first chapter of this thesis, we will briefly outline the theory of quantum elastic scattering, and the relation between the cross section and the exact stationary solutions of the problem.
In the second chapter, we will use the Wentzel–Kramers–Brillouin (WKB) semiclassical approximation to analyze the problem in further detail.
In the last chapter, we will show how to numerically solve the time-dependent Schrödinger equation and we will study the behavior of the wavefunction during a resonant scattering event. The relation between this approach and the time-independent solution of the quantum elastic problem based on phase shifts, that is usually found in textbooks, will be discussed in detail.

Chapter 1

Introduction to the hydrogen-krypton scattering

In the first part of this Chapter there will be an introduction to the theory of elastic scattering and phase shifts will be dealt with in order to find the total cross section of a scattering problem.
Phase shifts will be calculated numerically for the hydrogen-krypton scattering using Numerov's method to integrate the Schrödinger equation.

1.1 Elastic (non-relativistic) scattering

Schrödinger equation for free particles can be solved exactly. The solutions are plane waves in the form:

$$\psi_{\mathbf{k}}(\mathbf{r}, t) = \frac{1}{(2\pi\hbar)^{3/2}} e^{i(\mathbf{k}\cdot\mathbf{r} - \omega_{\mathbf{k}} t)}, \tag{1.1}$$

where $\mathbf{k}$ is the wave vector, $\hbar$ is the Planck constant and $\omega_{\mathbf{k}}$ is the frequency:

$$\omega_{\mathbf{k}} = \frac{\hbar \mathbf{k}^2}{2m}. \tag{1.2}$$

With also a potential, there is no longer an easy solution and the physically relevant solutions can be found by using boundary conditions.
If the region where the potential $V(\mathbf{r})$ interacts is restricted, i.e. there is a short-ranged potential, then the scattering solution can be seen as a superposition of the free solution and a scattering part which is given by the potential and it is an outgoing spherical wave.

With a potential $V(\mathbf{r})$ the time-independent Schrödinger equation becomes:

$$\left(\frac{\hbar^2}{2m}\nabla^2 + E\right)\phi(\mathbf{r}) = V(\mathbf{r})\phi(\mathbf{r}). \tag{1.3}$$

Using the Green's function method, the last equation transforms into the integral form:

$$\phi(\mathbf{r}) = \phi_0(\mathbf{r}) + \int G(\mathbf{r},\mathbf{r}')\, V(\mathbf{r}')\, \phi(\mathbf{r}')\, d^3\mathbf{r}', \tag{1.4}$$

where $\phi_0(\mathbf{r})$ is the solution of the homogeneous equation (without potential $V(\mathbf{r})$) and the Green's function $G(\mathbf{r},\mathbf{r}')$ is the solution of the Helmholtz equation:

$$\left(\frac{\hbar^2}{2m}\nabla^2 + E\right)G(\mathbf{r},\mathbf{r}') = \delta(\mathbf{r}-\mathbf{r}'). \tag{1.5}$$

For this problem the Green's function is, as well known,

$$G(\mathbf{r},\mathbf{r}') = -\frac{2m}{\hbar^2}\frac{e^{\pm ik|\mathbf{r}-\mathbf{r}'|}}{4\pi|\mathbf{r}-\mathbf{r}'|}, \tag{1.6}$$

where $\mathbf{r}$ represents the point where the scattering wave is calculated and $\mathbf{r}'$ is the point where there is the interaction of the potential.
With a restricted potential and a large $\mathbf{r}$, the condition $|\mathbf{r}| \gg |\mathbf{r}'|$ is well satisfied, so it follows that:

$$|\mathbf{r}-\mathbf{r}'| \simeq r - \frac{\mathbf{r}\cdot\mathbf{r}'}{r} = r - \hat{r}\cdot\mathbf{r}'. \tag{1.7}$$

By using it in (1.4), the general solution becomes:

$$\underbrace{\phi_{\mathbf{k}}(\mathbf{r})}_{\text{Term 1}} = \frac{1}{(2\pi\hbar)^{3/2}}\Bigg[\underbrace{e^{i\mathbf{k}\cdot\mathbf{r}}}_{\text{Term 2}} + \underbrace{f(\mathbf{k},\mathbf{k}')\frac{e^{ikr}}{r}}_{\text{Term 3}}\Bigg]. \tag{1.8}$$

where $\mathbf{k}' := k\hat{r}$ and the **scattering amplitude** is defined as:

$$f(\mathbf{k},\mathbf{k}') := -\frac{\sqrt{2\pi}m}{\hbar^2}\int e^{-i\mathbf{k}'\cdot\mathbf{r}'}\, V(\mathbf{r}')\, \phi(\mathbf{r}')\, d^3\mathbf{r}'. \tag{1.9}$$

Let us define also the terms in (1.8):

$$\phi_{\text{sc}} := \phi_{\mathbf{k}}(\mathbf{r}), \tag{1.10}$$

$$\phi_{\text{in}} := \frac{1}{(2\pi\hbar)^{3/2}}e^{i\mathbf{k}\cdot\mathbf{r}}, \tag{1.11}$$

$$\phi_{\text{am}} := \frac{1}{(2\pi\hbar)^{3/2}}f(\mathbf{k},\mathbf{k}')\frac{e^{ikr}}{r}. \tag{1.12}$$

When the potential $V(\mathbf{r})$ is radial and depends only on $|\mathbf{r}|$, then the scattering amplitude is a function of k and of the angle:

$$\theta := \arccos\left(\frac{\mathbf{k}\cdot\mathbf{r}}{kr}\right). \tag{1.13}$$

From (1.8), the solution $\phi_{\mathbf{k}}(\mathbf{r})$ can be seen as a superposition of a plane wave ϕ_{in} and a scattering component ϕ_{am} that is formally equal to an outgoing spherical wave.

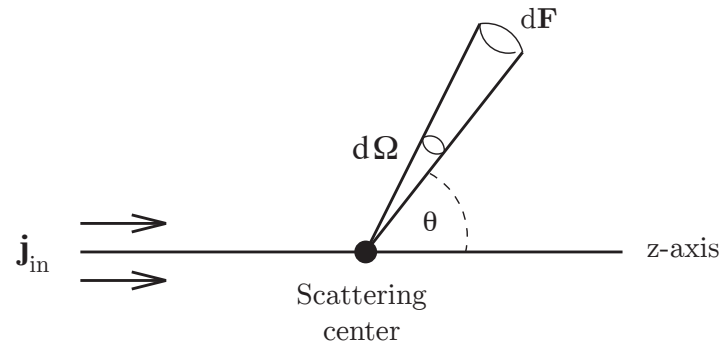

FIGURE 1.1: Explanation of the differential cross section

1.1.1 Differential Cross Section

In quantum mechanics a current of particles is written as

$$\mathbf{j} = \frac{\hbar}{2mi}\Big[\psi^*\nabla\psi - \psi\nabla\psi^*\Big], \tag{1.14}$$

and for example with a free particle it becomes:

$$\mathbf{j} = \frac{1}{(2\pi\hbar)^3}\frac{\hbar\,\mathbf{k}}{m}. \tag{1.15}$$

Experimentally one measures the probability current $\mathbf{j}_{\text{sc}} = \rho\mathbf{v}$ of particles which penetrate through the area

$$d\mathbf{F} = r^2 d\Omega\hat{r}, \tag{1.16}$$

where $d\Omega$ is the solid angle given by the resolution of the instrument and r is the distance from the scattering center (a schematic representation is shown in Figure 1.1).
This current is linked to the incoming current by the **differential cross section** that is defined as:

$$\frac{d\sigma}{d\Omega} := \frac{\mathbf{j}_{\text{sc}}\cdot d\mathbf{F}}{|\mathbf{j}_{\text{in}}|\,d\Omega} = \frac{\mathbf{j}_{\text{sc}}\cdot\hat{r}\;r^2}{|\mathbf{j}_{\text{in}}|}. \tag{1.17}$$

This definition of differential cross section can be also used in the previous quantum scattering problem, where $\mathbf{j}_{\text{in}}$ is given by (1.15) and $\mathbf{j}_{\text{sc}}$ needs to be calculated.
By using the definition (1.14), the radial part of $\mathbf{j}_{\text{sc}}$ becomes:

$$j^r_{\text{sc}} = \frac{1}{(2\pi\hbar)^3}\frac{\hbar\, k}{mr^2}|f(k,\theta)|^2, \tag{1.18}$$

that used in the scalar product with $d\mathbf{F}$ gives:

$$\mathbf{j}_{sc}\cdot d\mathbf{F} = \frac{1}{(2\pi\hbar)^3}\frac{\hbar\,\mathbf{k}}{m}|f(k,\theta)|^2 d\Omega. \tag{1.19}$$

So the differential cross section is:

$$\frac{d\sigma}{d\Omega} = |f(k,\theta)|^2. \tag{1.20}$$

1.1.2 Phase shifts

The definition of the **total cross section** is

$$\Sigma =: \int \frac{d\sigma}{d\Omega} d\Omega, \tag{1.21}$$

so it depends on the scattering amplitude.
When energy is fixed and $V(\mathbf{r})$ is rotationally symmetric, equation (1.8) depends only on θ, so the idea is to expand the three terms (1.10), (1.11) and (1.12) in a complete basis set of θ-wavefunctions, by focusing on the limit $r \to \infty$.

Term 1: Scattered wavefunction expansion – If $[\mathcal{H}, L^2] = 0$, the potential $V(\mathbf{r})$ is rotationally symmetric. Then, if $\mathbf{k}$ is set parallel to the z-axis, the angle θ of the spherical coordinate system is also the angle between $\mathbf{r}$ and $\mathbf{k}$ and the problem becomes ϕ-independent. In this case the solution of the time-independent Schrödinger equation is:

$$\phi_{\text{sc}}(r,\theta) = \sum_{l=0}^{\infty} \frac{u_l(r)}{r} P_l(\cos\theta), \tag{1.22}$$

where $P_l(\theta)$ are the Legendre functions. The radial and angular problems can be treated separately and the radial part of the Schrödinger equation takes the famous form:

$$\left[-\frac{\hbar^2}{2m}\frac{d^2}{dr^2} + V(r) + \frac{\hbar^2 l(l+1)}{2mr^2}\right] u_l(r) = E\, u_l(r). \tag{1.23}$$

In the region where $V(r) \simeq 0$, this equation has a general solution:

$$u_l(r) = B_l\, r\, j_l(kr) + C_l\, r\, \eta_l(kr), \tag{1.24}$$

where $j_l(kr)$ and $\eta_l(kr)$ are the Bessel and Neumann functions. They have the following asymptotic forms for $kr \gg 1$:

$$j_l(kr) \sim \frac{1}{kr}\sin\left(kr - \frac{l\pi}{2}\right), \tag{1.25}$$

$$\eta_l(kr) \sim -\frac{1}{kr}\cos\left(kr - \frac{l\pi}{2}\right), \tag{1.26}$$

and for $kr \ll 1$:

$$j_l(kr) \sim (kr)^l \tag{1.27}$$

$$\eta_l(kr) \sim -\frac{1}{(kr)^{l+1}} \tag{1.28}$$

Thus, the asymptotic behaviour of the radial scattering solution for $kr \gg 1$ is:

$$\frac{u_l(r)}{r} \sim B_l \frac{\sin(kr - \frac{l\pi}{2})}{kr} - C_l \frac{\cos(kr - \frac{l\pi}{2})}{kr} \tag{1.29}$$

or equivalently

$$\frac{u_l(r)}{r} \sim a_l \frac{\sin(kr - \frac{l\pi}{2} + \delta_l)}{kr} \tag{1.30}$$

where δ_l are called **phase shifts**.

Term 2: Free wavefunction expansion – For the homogeneous solution there is no longer a potential $V(\mathbf{r})$, so the solution is always of the type (1.24) but it cannot have the second term, because for $r \to 0$ the function $\eta_l(kr)$ is not integrable.
In this case the plane wave can be expanded as

$$\phi_{\text{in}} \propto \sum_{l=0}^{\infty} (i)^l (2l+1)\, j_l(kr)\, P_l(\cos\theta) \tag{1.31}$$

and it takes the following asymptotic form for $kr \gg 1$:

$$\phi_{\text{in}} \sim \sum_{l=0}^{\infty} (i)^l (2l+1)\, \frac{\sin(kr - \frac{l\pi}{2})}{kr}\, P_l(\cos\theta). \tag{1.32}$$

So the effect of the potential is a phase shift δ_l of the wavefunction with respect to the free wave solution.

Term 3: scattering amplitude expansion – The last part to expand is $f(\theta, k)$, but with the same basis set of wavefunctions the integral formulation transforms into an algebraic one:

$$f(k, \theta) = \sum_{l=0}^{\infty} f_l(k) P_l(\cos\theta), \tag{1.33}$$

where coefficients f_l depend on a_l and δ_l.

1.1.2.1 Total cross section and phase shifts

By using (1.30), (1.32) and (1.33), the comparison between the l-th partial wave on the left-hand side of (1.8) and that on the right-hand side gives the condition:

$$a_l \frac{\sin(kr - \frac{l\pi}{2} + \delta_l)}{kr} = (i)^l(2l+1)\frac{\sin(kr - \frac{l\pi}{2})}{kr} + \frac{e^{ikr}}{r} f_l. \tag{1.34}$$

With some calculations, it can be found that:

$$\begin{cases} a_l = (i)^l(2l+1)e^{i\delta_l} \\ f_l = \dfrac{2l+1}{k} e^{i\delta_l}\sin(\delta_l) \end{cases} \tag{1.35}$$

and the differential cross section can be written:

$$\frac{d\sigma}{d\Omega} = \frac{1}{k^2}\sum_{l\ l'}(2l+1)(2l'+1)\, e^{i(\delta_l - \delta_{l'})}\, \sin\delta_l \sin\delta_{l'}\, P_l(\cos\theta)\, P_{l'}(\cos\theta). \tag{1.36}$$

In this way the total cross section becomes:

$$\Sigma(E) = \frac{4\pi}{k^2}\sum_l (2l+1)\sin^2\delta_l, \tag{1.37}$$

where it has been used:

$$\int P_l(y)P_{l'}(y)dy = \frac{2}{2l+1}\delta_{l,l'}. \tag{1.38}$$

1.1.2.2 Numerical computation of phase shifts

In order to find phase shifts δ_l, the solution without the potential needs to be compared with the solution at large r in the presence of $V(r)$.
With a numerical approach this is not a problem because there are efficient methods that can solve the Schrödinger time-independent equation, like for example the Numerov's method [Gar14, pp. 35-36].
Now let us define:

$$\begin{aligned} \chi_l(r) := \frac{u_l(r)}{r} &\overset{kr\gg 1}{\simeq} a_l \frac{\sin(kr - \frac{l\pi}{2} + \delta_l)}{kr} \\ &= a_l \frac{\sin(kr - \frac{l\pi}{2})\cos(\delta_l) + \cos(kr - \frac{l\pi}{2})\sin(\delta_l)}{kr} \end{aligned} \tag{1.39}$$

and without the limit $kr \gg 1$, if $V(r) \simeq 0$, the wavefunction becomes:

$$\chi_l(r) \simeq a_l[j_l(kr)\cos\delta_l - \eta_l(kr)\sin\delta_l]. \tag{1.40}$$

Now, using (1.40), it is easy to prove that:

$$\tan\delta_l = \frac{j_l(kr_2) - \kappa j_l(kr_1)}{\eta_l(kr_2) - \kappa\eta_l(kr_1)}, \tag{1.41}$$

where

$$\kappa := \frac{\chi(r_2)}{\chi(r_1)}. \tag{1.42}$$

In conclusion, phase shifts δ_l and then total cross section can be computed by knowing the exact radial solution $\chi(r)$ and by using (1.41) and (1.42).

1.2 Hydrogen-krypton scattering

1.2.1 Reduced units

The hydrogen-krypton scattering is well described by a Lennard-Jones potential:

$$V(r) = 4\varepsilon\left[\left(\frac{\sigma}{r}\right)^{12} - \left(\frac{\sigma}{r}\right)^{6}\right], \tag{1.43}$$

with the following parameters:

$$\frac{\varepsilon_{\mathrm{H-Kr}}}{K_{\mathrm{B}}} = 68.505\,\mathrm{K},$$

$$\sigma_{\mathrm{H-Kr}} = 3.18\,\text{Å},$$

where K_{B} is the Boltzmann constant.
Now let us define a reduced unit of length $r = \bar{r}\cdot\sigma$ and one of energy $E = \bar{E}\cdot\varepsilon$. The reduced potential is defined as:

$$\bar{V}(r) := 4\varepsilon\left[\left(\frac{1}{r}\right)^{12} - \left(\frac{1}{r}\right)^{6}\right] \tag{1.44}$$

and it follows that:

$$V(r) = \bar{V}\left(\bar{r}\right). \tag{1.45}$$

In the same way the reduced wavefunction $\bar{\psi}$ will be

$$\bar{\psi}(\bar{r}) = \psi(r). \tag{1.46}$$

In the next paragraphs, reduced notation for functions will be omitted and, every time in a equation it will appear a reduced unit as an argument of a function, for an easier notation the reduced function $\bar{\psi}(\bar{r})$ will be written simply $\psi(\bar{r})$.
At last, let us introduce the dimensionless constant:

$$\zeta := \frac{\hbar^2}{2m\varepsilon\sigma^2}, \tag{1.47}$$

where m is the reduced mass of the system H-Kr.
This constant gives also an idea of how much classical or quantum the system is: for $\zeta \ll 1$ the system will be almost classical and in case of the H-Kr scattering its value is

$$\zeta_{\mathrm{H-Kr}} = 0.03517(1). \tag{1.48}$$

1.2.2 Numerov's algorithm

Numerov's method has been applied with the following parameters and considerations:

- the step $\delta\bar{r}$ has been chosen 10^{-5};
- the wavefunction has been computed from $\bar{r}_{\mathrm{start}} = 0.6$ to $\bar{r}_{\mathrm{stop}} = 20$; $\bar{r}_{\mathrm{start}}$ has not been chosen zero because in that point the potential is infinite, so, for a larger value as 0.6, there is no longer this problem and the final result does not change because for $\bar{r} < 0.6$ the wavefunction is almost null; instead $\bar{r}_{\mathrm{stop}}$ has been chosen large enough to ensure that the wavefunction can be considered approximately null at $\bar{r} > \bar{r}_{\mathrm{stop}}$.

The sum in (1.37) goes from 0 to ∞, but the algorithm stops when the following condition is satisfied:

$$\frac{|\Sigma^*_{L+1} - \Sigma^*_L|}{\Sigma^*_L} < 10^{-5} \qquad \text{where} \qquad \Sigma^*_L := \frac{4\pi}{k^2}\sum_{l=0}^{l=L}(2l+1)\sin^2\delta_l, \tag{1.49}$$

Final results can be seen in Figure 1.2 where the total cross section $\Sigma(E)$ is shown.

1.2.3 Resonances

In Figure 1.2, the total cross section Σ presents some spikes for specific energy values. This phenomenon is called **scattering resonance**. Experimental results are shown in Figure 1.3 [JPTW79, p. 614]. The similarity between the two plots confirms that the Lennard-Jones potential is a good model for the interaction between atoms involved in this problem.

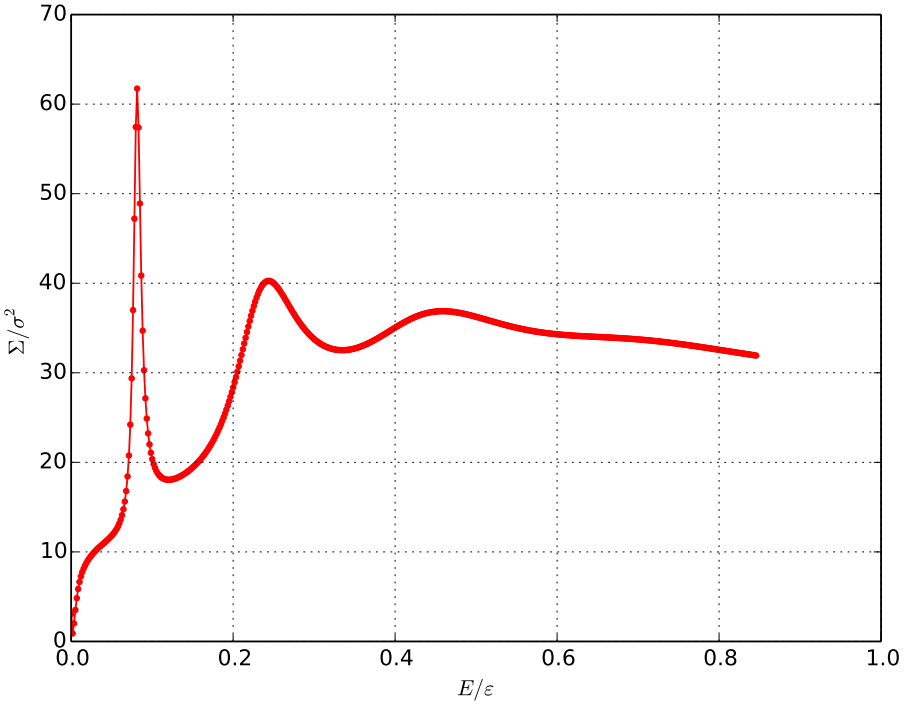

FIGURE 1.2: Total cross section Σ computed with Numerov's algorithm

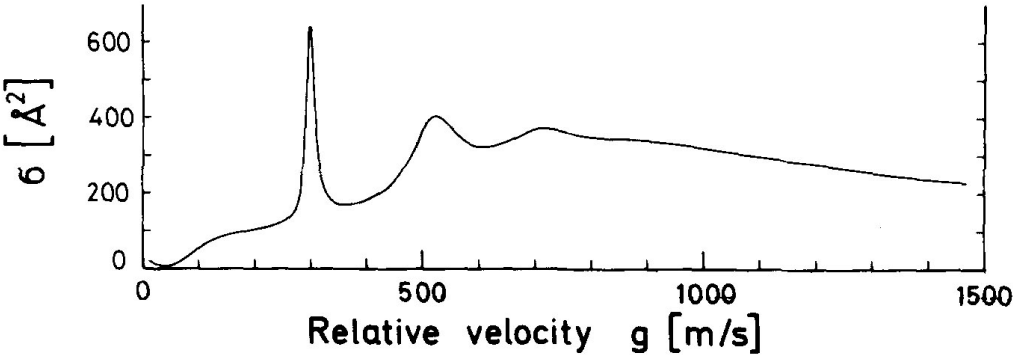

FIGURE 1.3: Experimental total cross section Σ for H-Kr scattering
[JPTW79, p. 618 fg. 3]

Chapter 2

The WKB theory

The Wentzel–Kramers–Brillouin (WKB) theory is a semiclassical approximation to the Schrödinger equation. In WKB theory, phase shifts can be expressed with an analytic formula, so there is not the necessity to solve numerically the Schrödinger equation.

In the first part of the chapter we will introduce the semiclassical approximation and then in the second and last part we will apply it to the hydrogen-krypton scattering.

2.1 An introduction to the WKB theory

2.1.1 A classical limit of quantum mechanics

Let us start from the time-dependent Schrödinger equation for a wavefunction ψ in the presence of a generic potential V:

$$i\hbar\frac{\partial\psi}{\partial t} = -\frac{\hbar^2}{2m}\nabla^2\psi + V\psi. \tag{2.1}$$

The limit $\hbar \to 0$ cannot be done, because the equation would become meaningless. In this limit the wavefunction of the quantum system begins to oscillate rapidly in the classically accessible regions and it is strongly damped in the classically forbidden regions; it is only the envelop of its squared norm that tends to a simple smooth function and represents the density of probability of finding the classical particle at a given position.
By proceeding in a slightly more complicated way, this problem can be solved with an approximation called WKB theory. It consists in parametrizing the wavefunction of the system as:

$$\psi(\mathbf{x}, t) = Ae^{\frac{i}{\hbar}S(\mathbf{x},t)}. \tag{2.2}$$

where $S(\mathbf{x}, t)$ is a complex function and A is a normalization coefficient.
With this solution the Schrödinger equation becomes:

$$-\frac{\partial S}{\partial t} = \frac{1}{2m}(\nabla S)^2 + V - \frac{i\hbar}{2m}\nabla^2 S, \tag{2.3}$$

that, if $\hbar \to 0$, takes the form:

$$-\frac{\partial S}{\partial t} = \frac{1}{2m}(\nabla S)^2 + V. \tag{2.4}$$

But this is formally identical to the Hamilton-Jacobi equation:

$$-\frac{\partial S}{\partial t} = \mathcal{H}(\mathbf{x}, \mathbf{p}), \tag{2.5}$$

where the arbitrary complex function S now corresponds to the Hamilton's principal function [Scr, pp. 1–7] and the momentum $\mathbf{p}$ to the gradient of it: $\mathbf{p} = \nabla S$.

The stationary situation

For a stationary state of definite energy E, the time-dependent wavefunction can be written as:

$$\psi(\mathbf{x}, t) = \phi(\mathbf{x}) e^{-\frac{i}{\hbar}Et}, \tag{2.6}$$

where $\phi(\mathbf{x})$ is the stationary wave function.
Also in this case, before discussing the classical limit $\hbar \to 0$, let us parametrize the stationary wave function as:

$$\phi(\mathbf{x}) = A e^{\frac{i}{\hbar}W(\mathbf{x})}, \tag{2.7}$$

and, by plugging this equation into the time-independent Schrödinger equation, one finds:

$$\frac{1}{2m}(\nabla W)^2 + V - \frac{i\hbar}{2m}\nabla^2 W = E, \tag{2.8}$$

that in the limit $\hbar \to 0$ becomes:

$$\frac{1}{2m}(\nabla W)^2 + V = E. \tag{2.9}$$

2.1.2 The validity of the classical approximation

Recalling equations (2.3) and (2.4), the limit $\hbar \to 0$ is reasonable only if the last term in (2.3) has a negligible effect with respect to other terms and in particular to the first.

This is equal to the condition $\hbar|\nabla^2 S| \ll (\nabla S)^2$ that can also be written as:

$$\hbar|\nabla \cdot \mathbf{p}| \ll \mathbf{p}^2. \tag{2.10}$$

In a one-dimensional problem it further simplifies to:

$$\frac{\hbar}{p^2}\left|\frac{dp}{dx}\right| \ll 1, \tag{2.11}$$

that in terms of the de Broglie wave length $\lambda\!\!\!^{-} := \hbar/p$ is

$$\left|\frac{d\lambda\!\!\!^{-}}{dx}\right| \ll 1. \tag{2.12}$$

Now, by using the following relations:

$$\frac{dp}{dt} = -\frac{dV}{dx}, \qquad p = \sqrt{2m(V-E)}, \tag{2.13}$$

the derivative of the momentum becomes:

$$\frac{dp}{dx} = -\frac{m}{p}\frac{dV}{dx}. \tag{2.14}$$

By plugging it into (2.11), the conclusion is:

$$\left|\frac{m\hbar}{p^3}\frac{dV}{dx}\right| \ll 1, \tag{2.15}$$

that, with the definition of a force $F := -dV/dx$, becomes:

$$|p| \gg |m\hbar F|^{1/3} \tag{2.16}$$

or in terms of the de Broglie length:

$$|\lambda\!\!\!^{-}| \ll \left|\frac{\hbar^2}{mF}\right|^{1/3}. \tag{2.17}$$

So the WKB approximation can be used only if the de Broglie wave length is smaller than a quantum-mechanical length scale of the system that depends on the mass, the force F and the Planck constant.

2.1.3 The semiclassical expansion for stationary states

Let us start from (2.8): by writing the solution W as a series expansion

$$W(\mathbf{x}) = W_0(\mathbf{x}) + (-i\hbar)W_1(\mathbf{x}) + (-i\hbar)^2 W_2(\mathbf{x}) + ..., \tag{2.18}$$

the resulting infinite system of coupled equations for the coefficients W_n is:

$$\begin{cases} (\nabla W_0)^2 = 2m(E-V) \\ \nabla W_0 \cdot \nabla W_1 + \dfrac{1}{2}\nabla^2 W_0 = 0 \\ (\nabla W_1)^2 + 2\nabla W_0 \cdot \nabla W_2 + \nabla^2 W_1 = 0 \\ \dots \end{cases} \tag{2.19}$$

If quantum effects are smaller than classical effects this expansion becomes useful because it can be restricted to the first two terms: $W \simeq W_0 - i\hbar W_1$.
In this case the corresponding wavefunction is:

$$\phi(\mathbf{x}) = A e^{W_1(\mathbf{x})} e^{\frac{i}{\hbar} W_0(\mathbf{x})}, \tag{2.20}$$

where W_0 determines the length scale on which the wavefunction oscillates or dies out, whereas W_1 controls the amplitude of the function.

One-dimensional problem – In this case the system (2.19) transforms into:

$$\begin{cases} \dot{W}_0^2 = p^2 \\ \dot{W}_0 \dot{W}_1 + \dfrac{1}{2}\ddot{W}_0 = 0 \end{cases} \tag{2.21}$$

and its exact general solution is:

$$\begin{cases} W_0(x) = \pm \displaystyle\int^x p(x')dx' + \kappa_1 \\ W_1(x) = -\ln\sqrt{p(x)} + \kappa_2 \end{cases} \tag{2.22}$$

where κ_1 and κ_2 are arbitrary constants, $p(x) := \sqrt{2m(E-V(x))}$ and integrals are indefinite.
So the semiclassical wavefunction ϕ has the following simple form:

$$\phi(x) \simeq \frac{A}{\sqrt{p(x)}} \exp\left[\pm \frac{i}{\hbar} \int^x p(x')dx' \right], \tag{2.23}$$

where the arbitrary normalization constant A includes the two previous constants of integration.

2.1.4 Behaviour of the semiclassical wavefunction in different regions

The two possible signs in (2.23) define two linearly independent solutions of the Schrödinger equation, so the general solution is given by the linear combination:

$$\phi(x) = \frac{B}{\sqrt{p(x)}}\exp\left[\frac{i}{\hbar}\int^x p(x')dx'\right] + \frac{C}{\sqrt{p(x)}}\exp\left[-\frac{i}{\hbar}\int^x p(x')dx'\right], \tag{2.24}$$

where B and C are arbitrary coefficients.

Classically allowed regions – In these regions where $E > V(x)$, $p(x)$ is real and positive and the semiclassical wave function becomes an oscillating function. Let us introduce the following quantum-mechanical wave number:

$$k(x) = \frac{p(x)}{\hbar} = \frac{1}{\hbar}\sqrt{2m[E - V(x)]}. \tag{2.25}$$

So the wavefunction can be written as:

$$\phi(x) = \frac{B_1}{\sqrt{k(x)}}\exp\left[i\int^x k(x')dx'\right] + \frac{C_1}{\sqrt{k(x)}}\exp\left[-i\int^x k(x')dx'\right] \tag{2.26}$$

or equivalently:

$$\phi(x) = \frac{D_1}{\sqrt{k(x)}}\sin\left[\int^x k(x')dx' + \delta\right]. \tag{2.27}$$

Classically forbidden regions – In this case $E < V(x)$ and $p(x)$ becomes imaginary. It is convenient to write the wave function in terms of a real quantum-mechanical penetration number $\beta(x)$:

$$\beta(x) := -\frac{i\,p(x)}{\hbar} = \frac{1}{\hbar}\sqrt{2m[V(x) - E]}. \tag{2.28}$$

In this way the general solution of this region becomes:

$$\phi(x) = \frac{B_2}{\sqrt{\beta(x)}}\exp\left[\int^x \beta(x')dx'\right] + \frac{C_2}{\sqrt{\beta(x)}}\exp\left[-\int^x \beta(x')dx'\right], \tag{2.29}$$

that is a superposition of decreasing and increasing real exponentials.

Classical turning points – In these points where $V(\bar{x}) = E$, the kinetic energy vanishes, $p(\bar{x})$ is zero and approach looses its validity.
In fact, close to these points, the semiclassical expansion is no longer valid because, when $p = 0$ and $F = -\frac{dV}{dx} \neq 0$, the condition (2.16) is no more respected.

2.1.5 Matching of wavefunctions

Without a form of the wavefunction in the regions close to the turning points, there is no way to match the oscillating wavefunction of the classically permitted regions and the exponential wavefunction of the classically forbidden regions.
If the potential is a sufficiently slowly varying function, it is possible to use another approximation in the neighbourhood of a turning point, called **linear potential approximation**.
By doing a first order expansion of the potential:

$$\begin{aligned} V(x) &\simeq V(\bar{x}) + V'(\bar{x})(x - \bar{x}) \\ &= E - F(\bar{x})(x - \bar{x}), \end{aligned} \tag{2.30}$$

the Schrödinger equation can be solved exactly.
In a region sufficiently close to a turning point where the linearization of the potential is a reliable approximation, the momentum $p(x)$ can be written as:

$$\begin{aligned} |p(x)| &\simeq |p'(x)(x - \bar{x})| \\ &\simeq \sqrt{2m|F(x)|\,|x - \bar{x}|}. \end{aligned} \tag{2.31}$$

Now, by using the necessary condition (2.16) and the definition of the de Broglie wave length, one finds the condition:

$$|x - \bar{x}| \ll \frac{1}{2}|\lambda\!\!\!^{-}(x)|, \tag{2.32}$$

that establishes when both approximations can be applied.

2.2 Resonances in the WKB theory

2.2.1 The radial problem

With a three-dimensional spherically symmetric problem like the H-Kr scattering, it is convenient to introduce an effective potential:

$$V_{\text{eff}}(r) = V(r) + \frac{\hbar^2 l(l+1)}{2mr^2}, \tag{2.33}$$

and the situation becomes formally equal to the one-dimensional problem discussed in the previous section, but with the following effective expressions that include the effects

of angular momentum:

$$\begin{cases} k_{\text{eff}}(r) = \dfrac{1}{\hbar}\sqrt{2m(E - V_{\text{eff}}(r))} \\ \beta_{\text{eff}}(r) = \dfrac{1}{\hbar}\sqrt{2m(V_{\text{eff}}(r) - E)} \end{cases} \tag{2.34}$$

If the potential is less singular than $1/r^2$ for $r \to 0$ and tends to zero for $r \to +\infty$, in the limit $r \to 0$ the problem is dominated by the centrifugal term and it follows that:

$$|\lambda\!\!\!^{-}_{\text{eff}}| = \frac{1}{|k_{\text{eff}}|} \simeq \frac{r}{\sqrt{l(l+1)}}. \tag{2.35}$$

The condition (2.12) then implies:

$$l \gg 1. \tag{2.36}$$

So the semiclassical approximation holds true when this condition is satisfied, however if the term in the potential with $l(l+1)$ is changed into $(l+1/2)^2$ (this is called **Langer modification**), the accuracy of the results can be further improved.
This modification is clearly irrelevant in the limit of large l, where the semiclassical approximation is a priori expected to be reliable, but improves the results for small values of l.

2.2.2 Resonances

Now let us focus on the effective potential $V_{\text{eff}}(r)$ shown in Figure 2.1 that satisfies:

$$\lim_{r\to 0} V_{\text{eff}}(r) = +\infty \qquad\qquad \lim_{r\to\infty} V_{\text{eff}}(r) = 0 \tag{2.37}$$

and presents a finite well followed by a finite barrier on the right-side.
With the energy shown in the Figure, there are three classical turning points called r_1, r_2 and r_3. The following regions:

$$II =]r_1, r_2[\qquad \text{and} \qquad IV =]r_3, +\infty[\tag{2.38}$$

are classically allowed, whereas

$$I =]0, r_1[\qquad \text{and} \qquad III =]r_2, r_3[\tag{2.39}$$

are classically forbidden.
At last, let us introduce the following parameters that describe the well and the finite barrier:

$$J = \int_{r_1}^{r_2} k_{\text{eff}}(r')dr' \tag{2.40}$$

$$K = \int_{r_2}^{r_3} \beta_{\text{eff}}(r')dr'. \tag{2.41}$$

Metastable quasi-stationary states and decay

In a decay situation the wave function vanishes at the origin and consists only in a progressive wave at infinity; from a quantitative point of view, this means that in the region IV the wavefunction will be of the type (2.26), but without the term with the coefficient C_1.
By matching the wavefunctions between classically permitted regions and classically forbidden regions, the general form of the wavefunction becomes: [Scr, p. 80]:

$$\begin{cases} u_l^I(r) & \simeq \dfrac{C_l}{2\sqrt{\beta_{\text{eff}}(r)}} \exp\left(-\displaystyle\int_r^{r_1} \beta_{\text{eff}}(r')dr' \right) \\ u_l^{II}(r) & \simeq \dfrac{C_l}{\sqrt{k_{\text{eff}}(r)}} \sin\left(\displaystyle\int_{r_1}^{r} k_{\text{eff}}(r')dr' + \frac{\pi}{4} \right) \\ u_l^{III}(r) & \simeq \dfrac{(-1)^n C_l}{2\sqrt{\beta_{\text{eff}}(r)}} \left[\exp\left(-\displaystyle\int_{r_2}^{r} \beta_{\text{eff}}(r')dr' \right) + \frac{i}{2} e^{-2K} \left(\displaystyle\int_{r_2}^{r} \beta_{\text{eff}}(r')dr' \right) \right] \\ u_l^{IV}(r) & \simeq \dfrac{(-1)^n C_l}{2\sqrt{k_{\text{eff}}(r)}} \left[e^{i\frac{\pi}{4}} e^{-K} \exp\left(i \displaystyle\int_{r_3}^{r} k_{\text{eff}}(r')dr' \right) \right], \end{cases} \tag{2.42}$$

and there is also the following quantization condition:

$$J = \left(n + \frac{1}{2} \right) \pi - \frac{i}{2} \log\left(\frac{1 - \frac{1}{4} e^{-2K}}{1 + \frac{1}{4} e^{-2K}} \right). \tag{2.43}$$

The last condition, if $K \gg 1$, simplifies to:

$$J \simeq \left(n + \frac{1}{2} \right) \pi - \frac{i}{4} e^{-2K} \tag{2.44}$$

and it cannot be satisfied if J is real. But if J has to be a complex value, also the energy E must be complex.

Complex energies – The time evolution of a stationary state $\phi(\mathbf{x})$ with fixed energy E is:

$$\psi(\mathbf{x}, t) = \phi(\mathbf{x})\, e^{-i\frac{E}{\hbar}t}. \tag{2.45}$$

If the energy $E = E_0 - i\Gamma/2$ is complex, then the squared modulus of the time-dependent wavefunction becomes:

$$|\psi(\mathbf{x}, t)|^2 = |\phi(\mathbf{x})|^2\, e^{-\frac{\Gamma t}{\hbar}}, \tag{2.46}$$

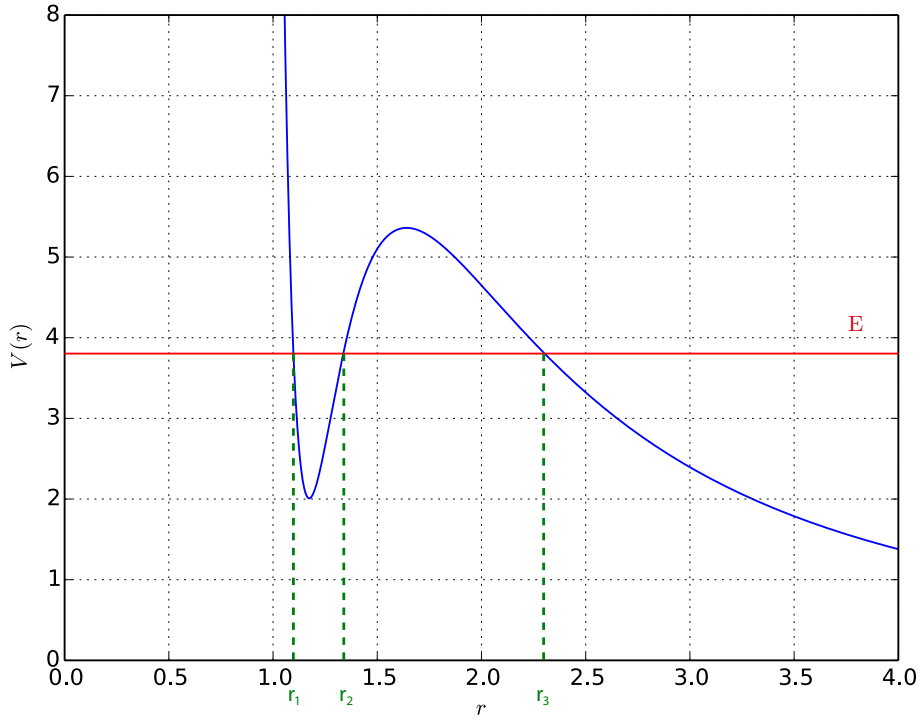

FIGURE 2.1: Resonant effective potential $V_{\text{eff}}(r)$

that is formally equal to a problem of decay where $\Gamma/2$ represents the decay rate and the lifetime of the state is:

$$\tau := \frac{2\hbar}{\Gamma}. \tag{2.47}$$

With complex energies, the quantization condition (2.44) can be written as:

$$\begin{cases} J|_{E_0} = \left(n + \dfrac{1}{2}\right)\pi \\ \Gamma = \dfrac{1}{2}\left(\dfrac{\partial J}{\partial E}\right)^{-1}_{E_0} e^{-2K}. \end{cases} \tag{2.48}$$

The scattering problem

The other possible situation is a scattering problem, in which case the external region has also a regressive wave and, focusing on the case $K \gg 1$, the wavefunction becomes:

$$\begin{cases} u_l^I(r) \simeq \dfrac{C_l}{2\sqrt{\beta_{\text{eff}}(r)}} \exp\left(-\displaystyle\int_r^{r_1} \beta_{\text{eff}}(r')dr' \right) \\ u_l^{II}(r) \simeq \dfrac{C_l}{\sqrt{k_{\text{eff}}(r)}} \sin\left(\displaystyle\int_{r_1}^{r} k_{\text{eff}}(r')dr' + \frac{\pi}{4} \right) \\ u_l^{III}(r) \simeq \dfrac{C_l}{2\sqrt{\beta_{\text{eff}}(r)}} \left[\sin J \exp\left\{ -\displaystyle\int_{r_2}^{r} \beta_{\text{eff}}(r')dr' \right\} + 2\cos J \exp\left\{ -\displaystyle\int_{r_2}^{r} \beta_{\text{eff}}(r')dr' \right\} \right] \\ u_l^{IV}(r) \simeq \dfrac{C_l}{\sqrt{k_{\text{eff}}(r)}} \left[e^{-i\frac{\pi}{4}} \left(\cos J\, e^K + \frac{i}{4} \sin J\, e^{-K} \right) \exp\left\{ i \displaystyle\int_{r_3}^{r} k_{\text{eff}}(r')dr' \right\} + \right. \\ \qquad \left. + e^{i\frac{\pi}{4}} \left(\cos J\, e^K - \frac{i}{4} \sin J\, e^{-K} \right) \exp\left\{ -i \displaystyle\int_{r_3}^{r} k_{\text{eff}}(r')dr' \right\} \right]. \end{cases} \tag{2.49}$$

There is no longer a complex condition, because the regressive component in the region IV is no more forced to be zero: now there is a radial wave coming in from $r \to \infty$ and a radial wave getting out to $r \to \infty$.

Phase shifts in WKB – For large r the wave function can be written in the following way:

$$u_l(r) \propto \sin\left[\int_{r_3}^{r} k_{\text{eff}}(r')dr' + \frac{\pi}{4} + \arg\left(\cot J + \frac{i}{4} e^{-2K} \right) \right] \tag{2.50}$$

Let us now study the case without the presence of the potential. The effective potential becomes exactly the radial part and there is only one turning point (Figure 2.2). By using the Langer modification, the wavefunction in the classically permitted region becomes:

$$u_l^{II}(r) \simeq \frac{C_l}{\sqrt{k_{\text{eff}}\big|_0(r)}} \sin\left(\int_{r_0}^{r} k_{\text{eff}}(r')dr' \Big|_0 + \frac{\pi}{4} \right), \tag{2.51}$$

where, without the potential:

$$k_{\text{eff}}(r)\big|_0 = \sqrt{k^2 - \frac{(l+1/2)^2}{r^2}}. \tag{2.52}$$

This quantity vanishes in the classical turning point r_0:

$$r_0 = \frac{l + \frac{1}{2}}{k} \tag{2.53}$$

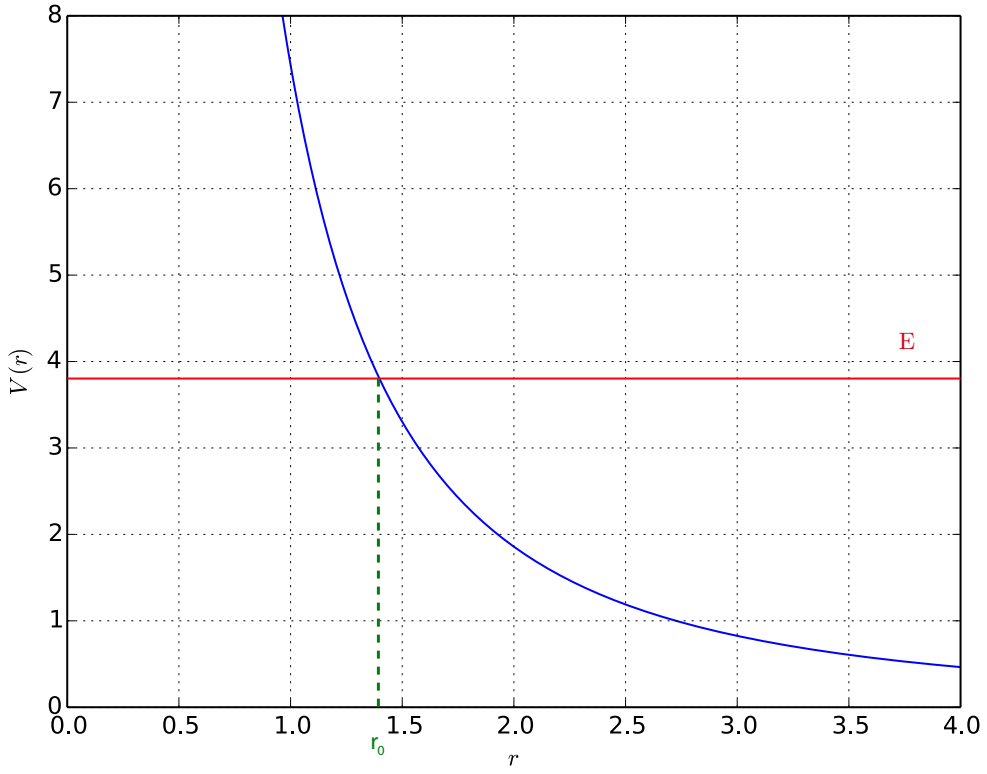

FIGURE 2.2: Effective potential without $V(r)$

and, if $r \gg r_0$, then:

$$\begin{aligned}\int_{r_0}^{r} k_{\text{eff}}(r')dr'\Big|_0 &= k\left[\sqrt{(r')^2 - r_0^2} - r_0 \arccos\left(\frac{r_0}{r'}\right)\right]_{r_0}^{r} \\ &\simeq k\left[r - r_0\frac{\pi}{2}\right] \\ &\simeq kr - l\frac{\pi}{2} - \frac{\pi}{4}\end{aligned} \tag{2.54}$$

and the wave function becomes:

$$u_l(r)\big|_0 \propto \sin\left(kr - l\frac{\pi}{2}\right), \qquad r \gg r_0. \tag{2.55}$$

In the presence of a general potential $V(r)$, the last equations transform into

$$k_{\text{eff}}(r)\big|_V = \sqrt{k^2 - \frac{2m}{\hbar^2}V(r) - \frac{(l+1/2)^2}{r^2}}. \tag{2.56}$$

$$\int_{r_0}^{r} k_{\text{eff}}(r')dr'\Big|_V \simeq kr - l\frac{\pi}{2} - \frac{\pi}{4} + \delta_l \tag{2.57}$$

$$u_l(r)\big|_V \propto \sin\left(kr - l\frac{\pi}{2} + \delta_l\right), \qquad r \gg r_0. \tag{2.58}$$

With a potential that presents a finite well and a finite barrier, the phase shifts δ_l become the sum of two terms (see 2.50):

$$\delta_l = \delta_l^{\text{nor}} + \delta_l^{\text{res}}, \tag{2.59}$$

where the first one is given by the direct reflection on the finite barrier:

$$\delta_l^{\text{nor}} = \int_{r_3}^{r} k_{\text{eff}}(r')dr'\Big|_0^V, \tag{2.60}$$

whereas the second term is due to the possibility of tunnelling and represents an extra effect that can show a resonance phenomenon:

$$\delta_l^{\text{res}} = \arg\left(\cot J + \frac{i}{4}e^{-2K}\right). \tag{2.61}$$

2.2.3 Conclusions

It can be proved [Scr, pp. 83–84] that δ_l^{res} begins to rise when we consider an energy close to E_0, where E_0 is the real part of the discrete energies found in the decay-metastable problem.

This is the prove that the decay-situation and the scattering-situation are only two ways to study the same problem.

2.3 Application to the hydrogen-krypton scattering

2.3.1 H-Kr scattering

In a scattering situation a wave packet comes from $r \to \infty$ and hits the potential barrier.

With the semiclassical approximation there are two ways to compute phase shifts: equations (1.41) and (1.42) can be used with the wavefunction at large r described in (3.11); otherwise phase shifts can be found with the analytical formulae (2.60) and (2.61).
As expected the two different methods give the same final total cross section Σ. To compute quantities (1.41) and (1.42), let us use the following algorithms:

- Newton-Raphson algorithm to find the turning points of the system with a relative precision of 10^{-6};

- basic algorithm to compute finite integrals like the trapezoidal rule with a step of 10^{-5}.

Final results are shown in Figure 2.3.

Discontinuities in Σ

As can be seen in Figure 2.3, the total cross section Σ presents some discontinuities. The effective potential for $l = 6$ presents a finite well and a finite barrier (Figure 2.4) and in some situation there can be three classical turning points (*Situation A*). In another example with $l = 9$, there is only one turning point (*Situation B*).
The type of *Situation* depends also on the total energy E of the system: in Figures 2.5, 2.6 and 2.7 there are shown some examples with $l = 6$ (green regions are the classically permitted regions and red regions are classically forbidden).
In WKB theory *Situation A* is different from *Situation B*, because the number of classical regions is different and so there are different conditions to merge the wavefunctions.

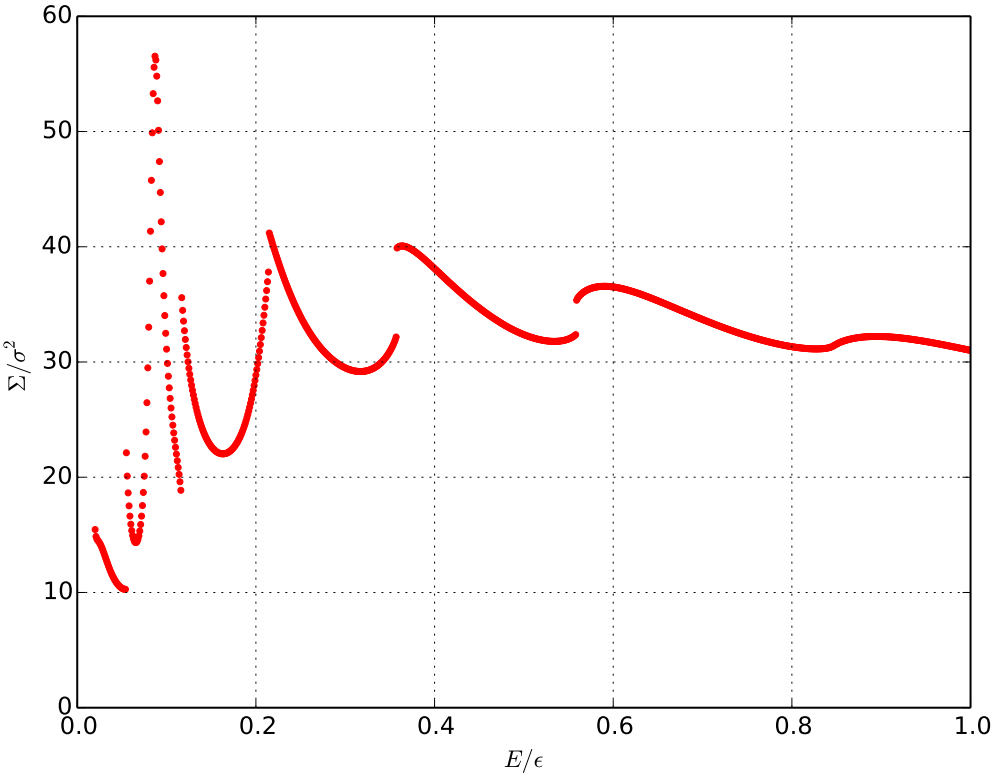

FIGURE 2.3: Total cross section computed with the WKB theory

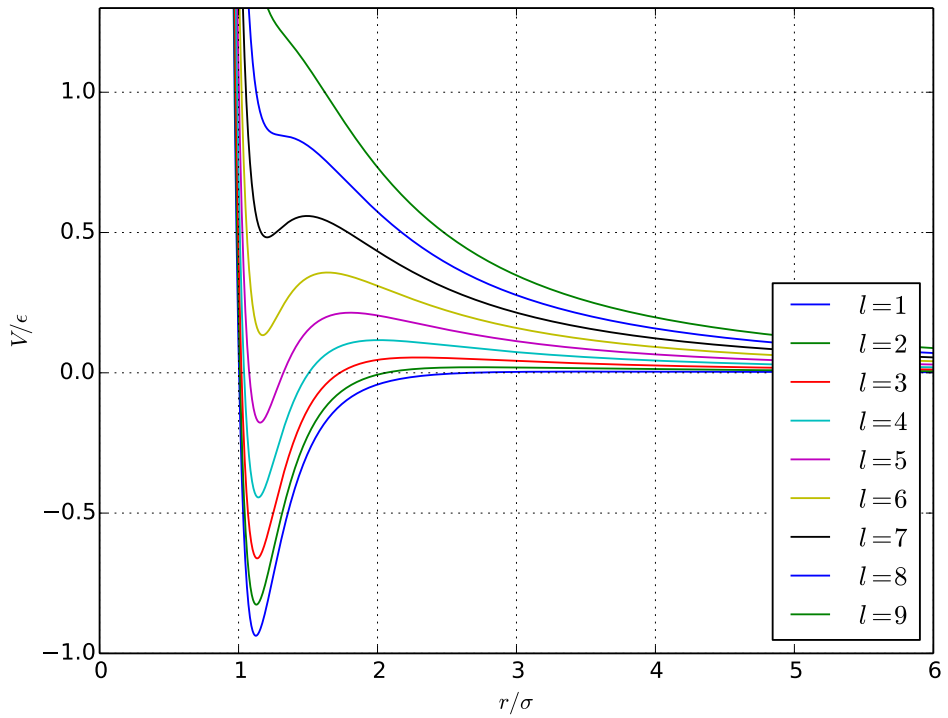

FIGURE 2.4: Lennard-Jones potential plus the radial part, varying the quantum number l

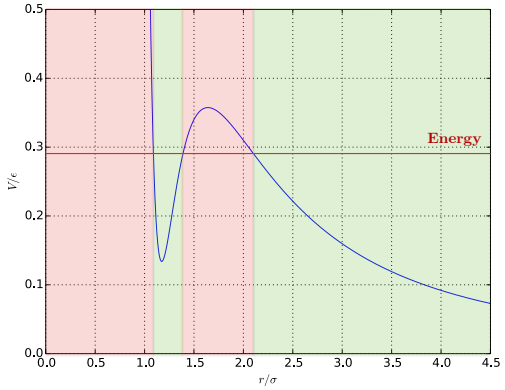

FIGURE 2.5: *Situation A* example 1. Phase shifts terms: δ_l^{nor} and δ_l^{res}

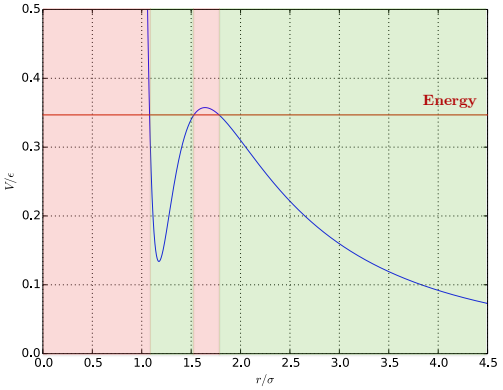

FIGURE 2.6: *Situation A* example 2. Phase shifts terms: δ_l^{nor} and δ_l^{res}

The energy E_{max} of the local maximum in the effective potential for $l = 6$ (see Figure 2.8) is perfectly equal to one of the energies where there is a discontinuity in the total cross section Σ (Figure 2.9).

So the term δ_l^{res} does not raise enough to compensate the gap between δ_l^{nor} computed in the *Situation A* when $E < E_{\text{max}}$ and δ_l^{nor} calculated in *Situation B* when $E > E_{\text{max}}$. A

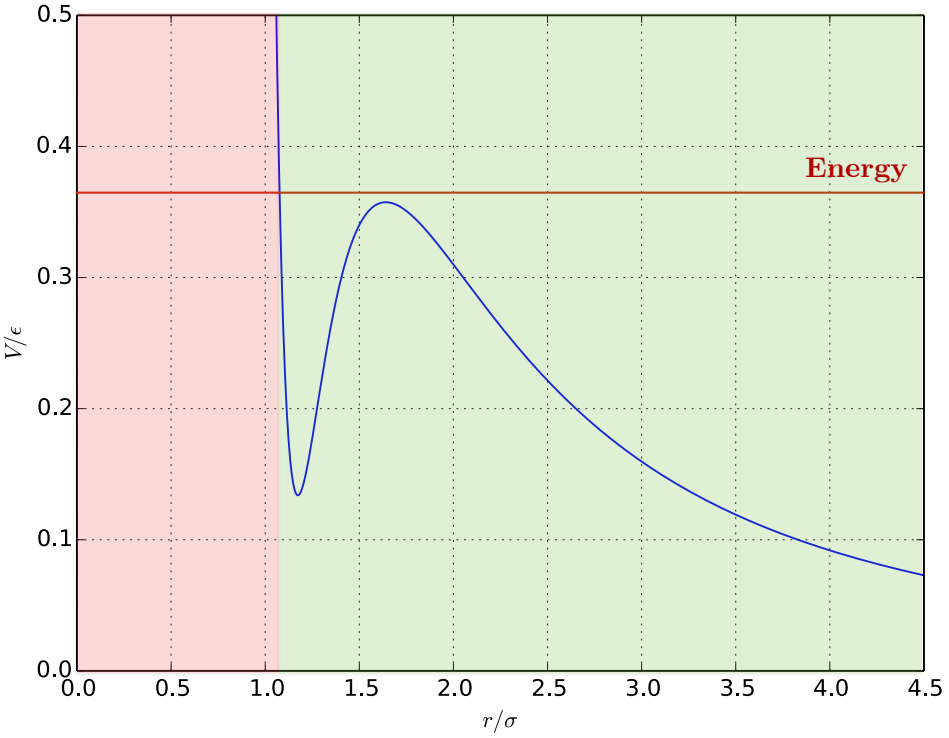

FIGURE 2.7: *Situation B* – In the phase shifts there is only the term δ_l^{nor}

possible explanation is that if $E \to E_{\max}$, then K is computed in a region close to two turning points where the semiclassical approximation is no longer valid.

Comparison of the first resonance

But the WKB theory is not even totally wrong, indeed plots in Figure 2.3 and 1.2 show the same order of magnitude and approximately the same first resonance spike.
The resonant component, for the first resonance, is $l = 4$ as can be seen in Figure 2.10, where there are shown the components of the total cross section Σ for each value of l, i.e. the single terms of the sum in (1.37). This is compatible with the exact solution computed with the Numerov's algorithm and the two results are compared in Figure 2.11.
It can be proved [Scr, pp. 84] that the partial scattering amplitude f_l for energies close to a resonance E_0 has the following behaviour:

$$|f_l(E)|^2 \propto \frac{1}{(E - E_0)^2 + \left(\frac{\Gamma}{2}\right)^2}. \tag{2.62}$$

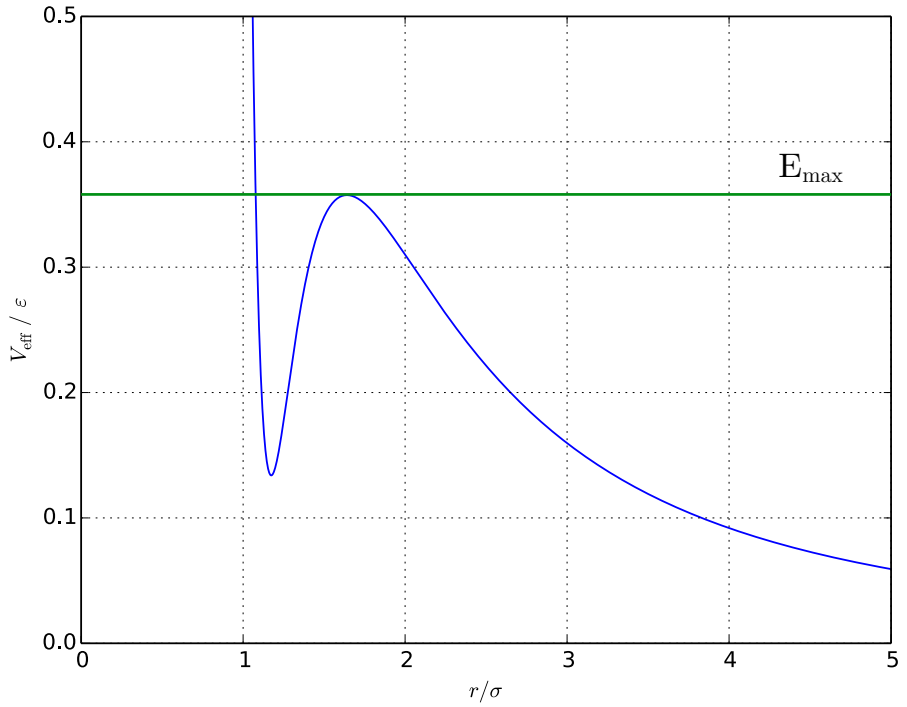

FIGURE 2.8: Local maximum in the effective potential

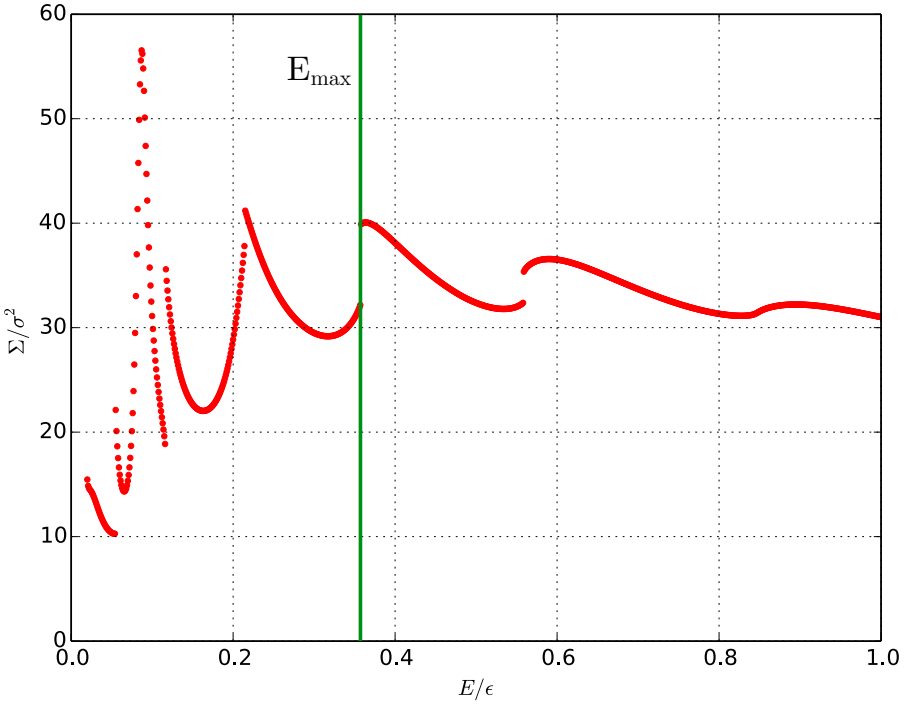

FIGURE 2.9: Discontinuity in the total cross section

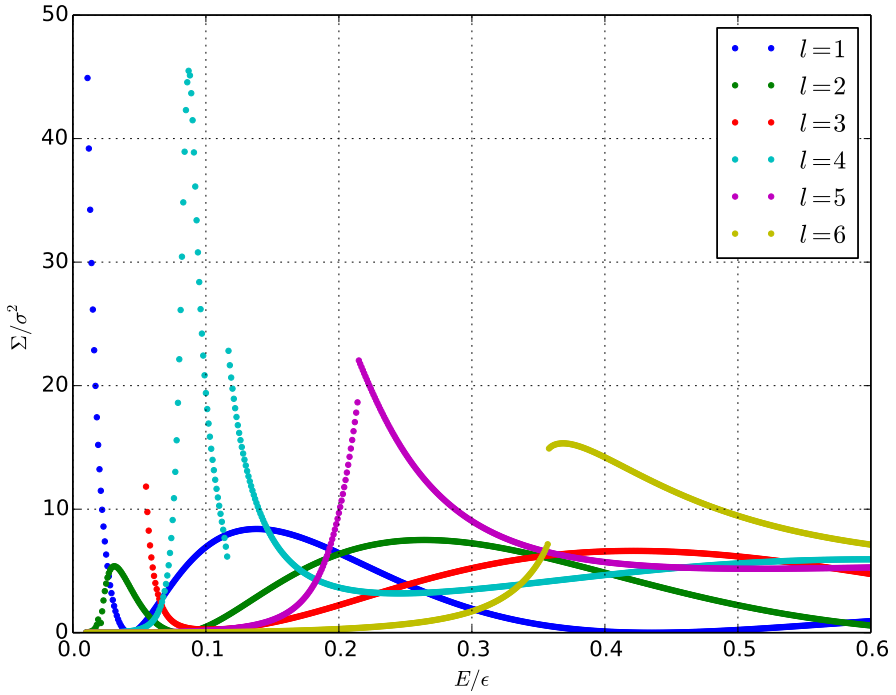

FIGURE 2.10: Partial cross sections for some quantum numbers l

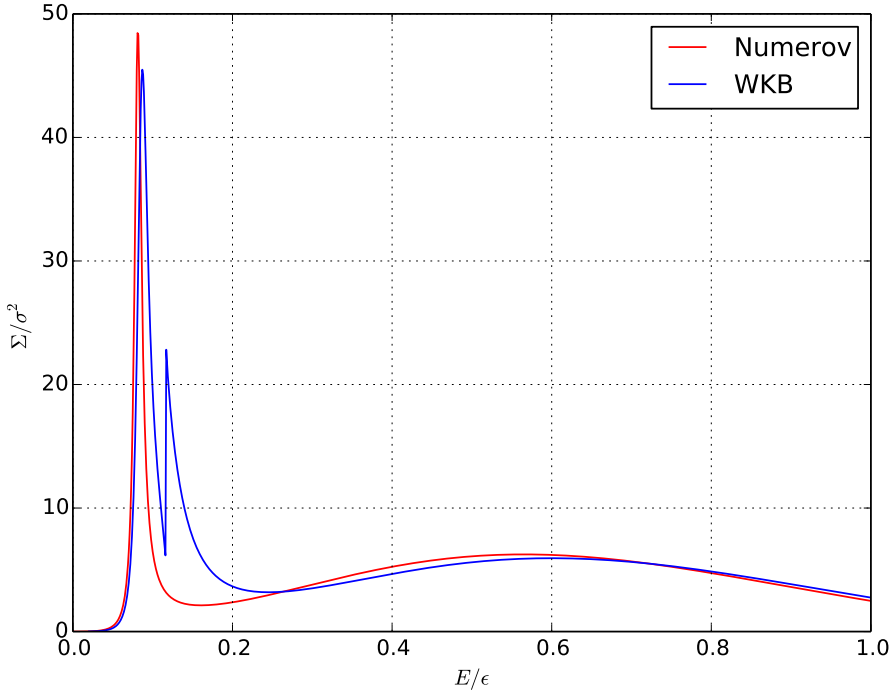

FIGURE 2.11: Component of the total cross section for $l = 4$, computed with WKB theory and the exact solution

	WKB theory fit	Exact solution fit
E_0/ε	0.08719(5)	0.08144(6)
Γ/ε	0.0176(5)	0.0112(1)

TABLE 2.1: First resonance comparison – E_0 and Γ are computed with a fit of the component for $l = 4$ of the total cross section with the line shape (2.62)

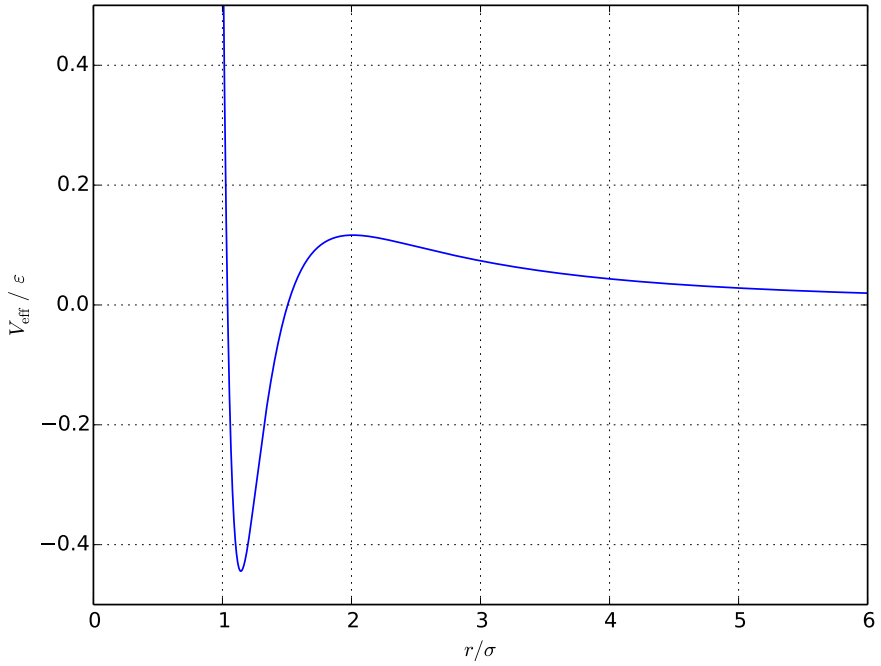

FIGURE 2.12: Effective potential for $l = 4$

The values of the parameters E_0 and Γ shown in Table 2.1 are computed by using the previous formula to fit the plots in Figure 2.11.
The conclusion is that the WKB theory gives only an idea of where the first resonance is, but it is not able to give a precise value. Evidently its approximations prevent to solve correctly the specific problem of H-Kr scattering.

2.3.2 Decay in WKB theory and the complex condition

Let us consider a decay situation with the effective potential $V_{\text{eff}}(r)$ for $l = 4$ and let us define the following complex function:

$$h(E) = J - \left(n + \frac{1}{2}\right)\pi + \frac{i}{2}\log\left(\frac{1 - \frac{1}{4}e^{-2K}}{1 + \frac{1}{4}e^{-2K}}\right) \in \mathbb{C} \qquad \text{where} \qquad E \in \mathbb{C}. \tag{2.63}$$

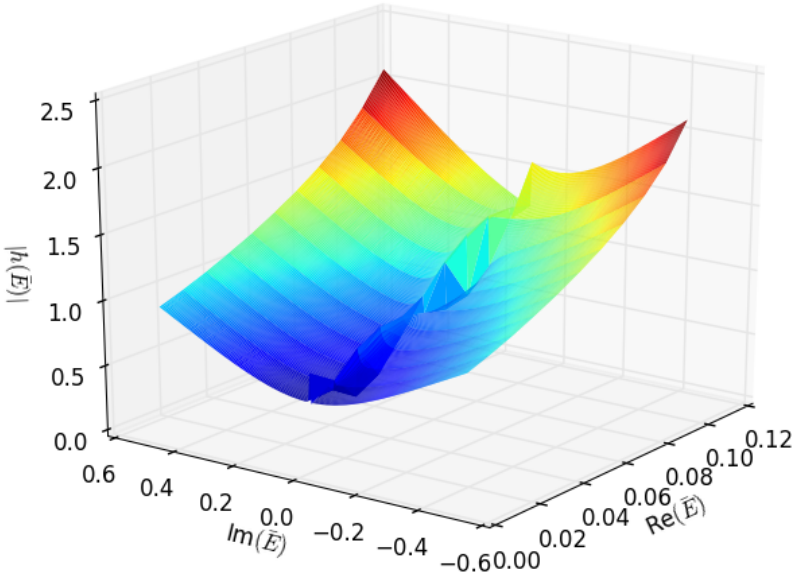

FIGURE 2.13: Modulus of the complex function $h(E)$

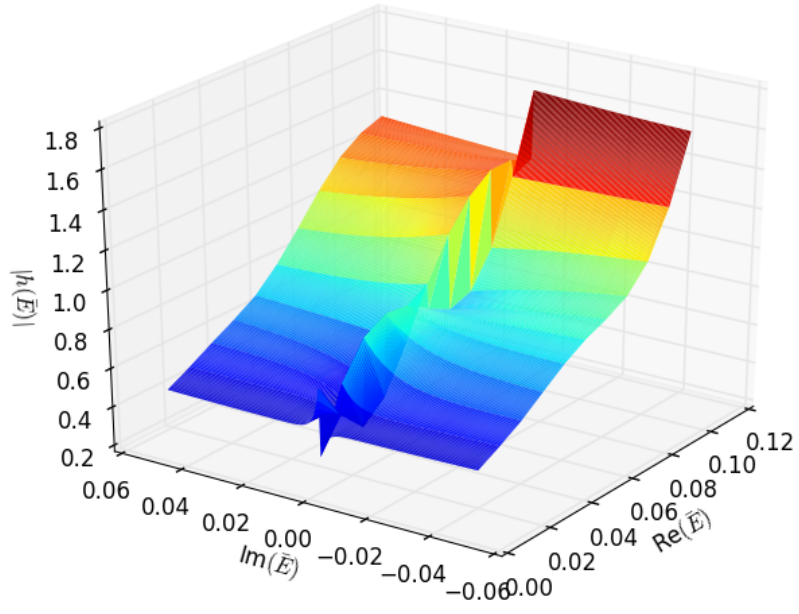

FIGURE 2.14: Modulus of the complex function $h(E)$

Its roots $\{\tilde{E} : |h(\tilde{E})| = 0\}$ are solutions of the complex condition (2.43).
Newton-Raphson is not the most efficient algorithm to find complex roots, but it is also very simple to implement. As starting point the algorithm needs a complex number near to the desired root and for the first resonance the value of the fit of the exact solution shown in Table 2.1 can be used.

The complex condition (2.43) looses its validity if there are not three classical turning points. So, as can be seen in Figure 2.12, the energy E_0 of the system has to satisfy:

$$E_0 \in [0, E_{\max}] \qquad \text{where} \qquad E_{\max} = 0.1165(1). \tag{2.64}$$

The result is that Newton-Raphson cannot find a solution for the complex condition (2.43), because the complex function $h(E)$ does not present any root in the range of energy (2.64) (Figures 2.13 and 2.14). So the complex condition of the WKB theory is not able to find the first resonance of the hydrogen-krypton scattering.
As shown in Figure 2.14, the function $h(E)$ presents also a discontinuity between the region where $\mathrm{Im}(E) > 0$ and the one where $\mathrm{Im}(E) < 0$ and this is another indication of the fact that the WKB is not a good approximation for solving the H-Kr scattering problem and for a time-independent study of the problem is necessary an exact solution.

Chapter 3

The time-dependent investigation

In this chapter the hydrogen-krypton scattering will be analysed with a time-dependent approach.
The first part will be an introduction to the split-operator's method and to the fast Fourier transform techniques for solving the time-dependent Schrödinger equation.
Then the scattering of a Gaussian wave packet and the decay of a metastable state focusing on the specific system H-Kr will be studied in detail. Finite size effects will be dealt with using an imaginary potential to avoid spurious reflections of the wavefunction.

3.1 Introduction to the time-dependent problem

3.1.1 Split-operator method

The time-dependent Schrödinger equation is

$$i\hbar\frac{\partial\psi}{\partial t} = \mathcal{H}\psi \tag{3.1}$$

where $\mathcal{H}$ is the Hamiltonian operator. It can be rewritten in

$$\psi(\mathbf{x},t) = \exp\left(-\frac{i\mathcal{H}t}{\hbar}\right)\psi_0(\mathbf{x}) \tag{3.2}$$

where $\psi_0(\mathbf{x})$ is the wavefunction at $t = 0$ that is given by the initial conditions.
Let us introduce also a reduced unit of time:

$$\bar{t} = t\frac{\varepsilon}{\hbar}. \tag{3.3}$$

In this way (3.2) simplifies to:

$$\psi(\bar{\mathbf{x}}, \bar{t}) = \exp\left(\frac{i\mathcal{H}\bar{t}}{\varepsilon}\right)\psi_0(\bar{\mathbf{x}}) = \exp\left[-i\bar{t}\zeta\,\nabla^2_{\bar{\mathbf{x}}} - i\bar{t}\,\frac{V(\bar{\mathbf{x}})}{\varepsilon}\right]\psi_0(\bar{\mathbf{x}}). \tag{3.4}$$

This expression can be written in the more useful way using the Trotter's formula [Gar14, p. 24]:

$$\psi(\bar{\mathbf{x}}, \bar{t}) = \lim_{\varrho\to\infty}\left[\exp\left(i\,\delta\bar{t}\,\zeta\,\nabla^2_{\bar{\mathbf{x}}}\right)\cdot\exp\left(-i\,\delta\bar{t}\,\frac{V(\bar{\mathbf{x}})}{\varepsilon}\right)\right]^{\varrho}\psi_0(\bar{\mathbf{x}}), \tag{3.5}$$

where $\delta\bar{t} = \bar{t}/\varrho$.

With a radial one-dimensional problem the last expression becomes:

$$u_l(\bar{r}, \bar{t}) = \lim_{\varrho\to\infty}\left[\exp\left(i\,\delta\bar{t}\,\zeta\,\frac{\partial^2}{\partial\bar{r}^2}\right)\cdot\exp\left(-i\,\delta\bar{t}\,\frac{V_{\text{eff}}(\bar{r})}{\varepsilon}\right)\right]^{\varrho}u_l(\bar{r}, 0). \tag{3.6}$$

Discretization of the problem and DFT – The Fourier transform of a function $\psi(x,t)$ is defined as:

$$\phi(k,t) := \int_{\mathbb{R}}\psi(x,t)e^{-ikx}dx. \tag{3.7}$$

With a periodic function $\psi(x+L,t) = \psi(x,t)$, the discrete Fourier transform (DFT) is:

$$\phi_k = \sum_{n=0}^{N-1}\psi_n\exp\left(-i\frac{2\pi kn}{N}\right), \tag{3.8}$$

where the interval L has been discretized in N segments of length $dx = L/N$ and $\psi_n = \psi(n\cdot dx)$ are the discrete samples of $\psi(x)$.

Analogously the expression:

$$\psi_n = \frac{1}{N}\sum_{k=0}^{N-1}\phi_k\exp\left(i\frac{2\pi kn}{N}\right) \tag{3.9}$$

corresponds to the inverse discrete Fourier transform. There is a special algorithm found by Cooley and Tukey that provides an efficient computation of (3.8) and (3.9) when N is a power of two and it is called Fast Fourier Transform (FFT) [CT65].

Using DFTs, derivatives of periodic functions can be written as:

$$\left.\frac{d\psi}{dx}\right|_n = \sum_{k=0}^{N-1}\phi_k\Delta_k\exp\left(i\frac{2\pi nk}{N}\right), \tag{3.10}$$

where

$$\Delta_k := \begin{cases} i\dfrac{2\pi k}{L} & k \le \dfrac{N}{2} \\ i\dfrac{2\pi(N-k)}{L} & k > \dfrac{N}{2}. \end{cases} \tag{3.11}$$

Application to the split-operator method – In order to solve (3.6), the time evolution of the wavefunction can be seen as a series of infinitesimal evolutions generated by the operators:

$$\exp\left(i\,\delta\bar{t}\,\zeta\,\frac{\partial^2}{\partial\bar{r}^2}\right), \tag{3.12}$$

$$\exp\left(-i\,\delta\bar{t}\,\frac{V_{\text{eff}}(\bar{r})}{\varepsilon}\right), \tag{3.13}$$

applied to the initial wavefunction $u_l(\bar{r},0)$. The latter operator due to the potential is a simple phase factor, whereas the first operator due to the kinetic energy contains a second derivative that can be easily calculated in Fourier space using equation (3.10).

First, it is necessary to discretize the period L in N parts and to define:

$$\eta_n(\tau) := u_l(\bar{r}_n, \tau\,\delta\bar{t}), \tag{3.14}$$

where $\delta\bar{t}$ is the time step and τ is an integer index. Then $\eta_n(\tau)$ is multiplied by:

$$\rho_n := \exp\left(-i\,\delta\bar{t}\,\frac{V_{\text{eff}}(\bar{r}_n)}{\varepsilon}\right) \tag{3.15}$$

and the Fourier transform $\tilde{\varphi}_k(\tau)$ of this new function $\varphi_n(\tau) = \rho_n \cdot \eta_n(\tau)$ has to be multiplied by:

$$\xi_k := \exp\left(i\,\delta\bar{t}\,\zeta\,\Delta_k^2\right). \tag{3.16}$$

In this way the wavefunction $\varphi_n(\tau+1)$ is obtained by transforming back the reciprocal function $\tilde{\varphi}_k(\tau+1) = \xi_k \cdot \tilde{\varphi}_k(\tau)$ with an inverse discrete Fourier transform.

3.1.2 The imaginary potential

To apply the split-operator method to the hydrogen-krypton scattering problem, the radial potential needs to be periodic, but in H-Kr case V_{eff} tends to zero when $r \to \infty$ and tends to ∞ when $r \to 0$.

Symmetrical potential – A first possible solution is to set a maximum point $\bar{r} = L$ and then to mirror the potential with respect to this point as shown[1] in Figure 3.1; this solves the problem of the discontinuity in the potential, but it might introduce spurious effects.

Indeed, for example with a Gaussian wave packet that moves from right to left (green line in the Figure), the wave packet hits the left-hand potential barrier (region A) and

[1] From now on, the potential, that has the unit of an energy, and the modulus of the wavefunction will be often shown in the same Figure with only one y-axis that shows the reduced units of both quantities.

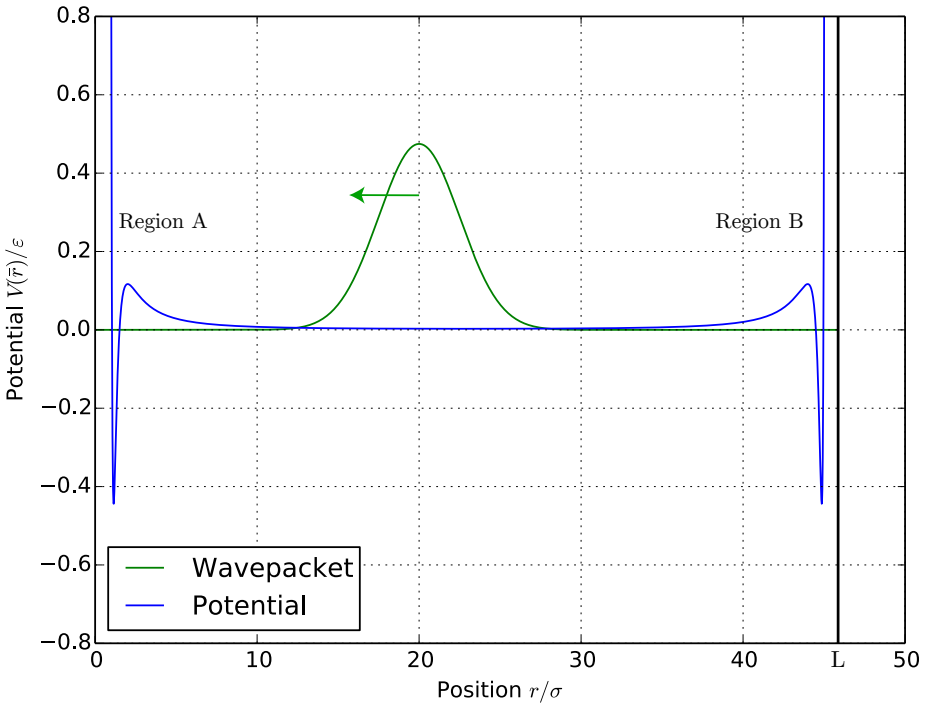

FIGURE 3.1: Qualitative representation of the mirrored potential

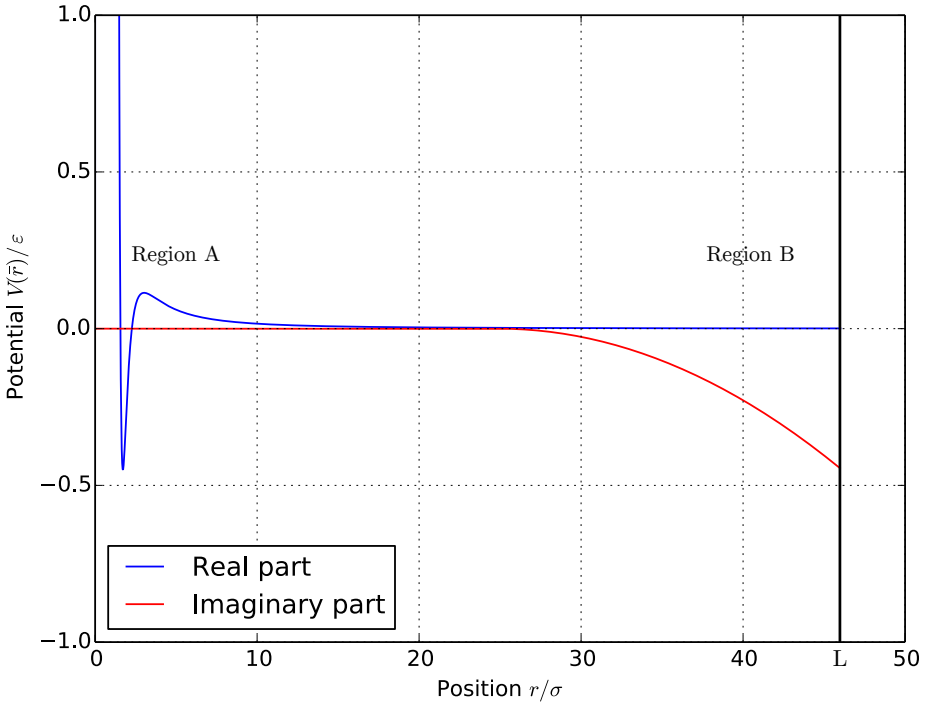

FIGURE 3.2: Qualitative representation of the complex potential

is reflected, but after some time the reflected part of the wave packet hits also the right-hand potential barrier (region B) and is again reflected.
This second reflection creates interferences that after a specific period of time T distorts the wavefunction in the region A and clearly compromises the results.

Imaginary potential – The other possibility is to add an imaginary component to the potential, even though this clearly does not have any physical meaning. In this way a third operator appears in the split-operator method and it is a real exponential:

$$\varrho_n := \exp\left(\delta\bar{t}\,\frac{V_{\text{imm}}(\bar{r})}{\varepsilon}\right). \tag{3.17}$$

In the region where the imaginary part of the potential is negative, the square modulus of the wavefunction is no longer conserved and decreases according to the equation (2.46) where now the decay rate Γ depends on the imaginary part of the potential V_{imm}.

In this way an imaginary negative potential can be added for large $\bar{r}$ near to L (as shown in Figure 3.2) and now, when a wave packet hits the potential barrier in region A and is reflected, the reflected component after some time enters in the region with the imaginary potential and vanishes.
The consequence is that

$$\mathcal{P}(t) = \int_0^L |u_l(r,t)|^2 dr \neq 1 \tag{3.18}$$

but this is not a problem because the interesting part will be what happens to the wavefunction in finite well of the region A.

3.2 The scattering of a Gaussian wave packet

Now let us focus on the effective hydrogen-krypton scattering potential with $l = 4$ and on an initial Gaussian wave packet of the form:

$$u_l(\bar{r}, \bar{t} = 0) \propto \exp\left(-\frac{(r - r_0)^2}{2\gamma^2}\right) \exp(i\bar{k}\bar{r}), \tag{3.19}$$

where γ is its width and $\bar{k} = k \cdot \sigma$ is the reduced wave vector that is negative because the packet comes from $\bar{r} \to \infty$.

3.2.1 The reciprocal wave packet

A wavefunction $\psi(r)$ has an average energy that is

$$\begin{aligned} \langle E \rangle &= \langle \psi | \mathcal{H} | \psi \rangle = \\ &= \langle E_{\text{kin}} \rangle + \langle \psi | V_{\text{eff}}(\bar{r}) | \psi \rangle. \end{aligned} \tag{3.20}$$

With the wave packet (3.19) it is possible to compute the mean kinetic energy analytically:

$$\begin{aligned} \frac{\langle E_{\text{kin}} \rangle}{\varepsilon} &= \left\langle u_l(\bar{r}, \bar{t}=0) \middle| -\zeta \frac{d^2}{d\bar{r}^2} \middle| u_l(\bar{r}, \bar{t}=0) \right\rangle = \\ &= \zeta \left(\bar{k}^2 + \frac{1}{\bar{\gamma}^2} \right). \end{aligned} \tag{3.21}$$

So the mean energy of a Gaussian wave packet depends on both k and γ and there are infinite combinations of these two values that gives the same $\langle E_{\text{kin}} \rangle$.

Every wavefunction can be seen as a superposition of an infinite number of plane waves and a plane wave with a reduced energy $\bar{E}$ has a corresponding wave vector that is:

$$\bar{k} = \sqrt{\frac{\bar{E}}{\zeta}}. \tag{3.22}$$

The Fourier transform of a Gaussian wave packet is itself a Gaussian wave packet and this reciprocal wave packet can be seen as an indication of which plane waves contribute more to the superposition.
So a *resonant* Gaussian wave packet will have a superposition of plane waves whose energies are close to E_{res} (Table 2.1).

In the reciprocal space, the Fourier transform of (3.19) is a Gaussian wave packet centered at $\bar{k}$ and with a width $1/\bar{\gamma}$.
The value Γ (see Table 2.1) has also a corresponding width in the k-space:

$$\delta\bar{k} = \sqrt{\frac{\bar{\Gamma}}{2\zeta}}. \tag{3.23}$$

So a Gaussian wave packet is a good *resonance* wavefunction if it has $k = k_{\text{res}}$ (see 3.22) and if its width γ meets the condition:

$$\sqrt{\frac{\bar{\Gamma}}{2\zeta}} \leq \frac{1}{\bar{\gamma}}. \tag{3.24}$$

3.2.2 What to expect and the permanence time

In particle colliders it is possible to reproduce experimentally a scattering experiment. In this field of experimental physics resonances appear for example when unstable particles are created only for some specific values of energy. One of the most famous examples is the delta baryon: the particle Δ_0 [HG07] has a rest mass of (1232 ± 2) MeV/c^2 and a really short mean lifetime:

$$(5.63 \pm 0.14) \cdot 10^{-24}\,\text{s}. \tag{3.25}$$

In quantum mechanics, the presence of the particle Δ^0 in these scattering experiments can be explained with the creation of a localized wavefunction in the region A (Figure 3.2) that is different from the initial scattered wave packet.

There is also a classical interpretation of resonances. In the classic version of the H-Kr scattering problem, the two atoms, abstracted as point-like particles, have an interaction described by the Lennard-Jones potential. For some specific energies of the system, the two atoms stay close together for a much longer time, as shown in Figure 3.3. This phenomenon is the classical interpretation of *resonance energy*.

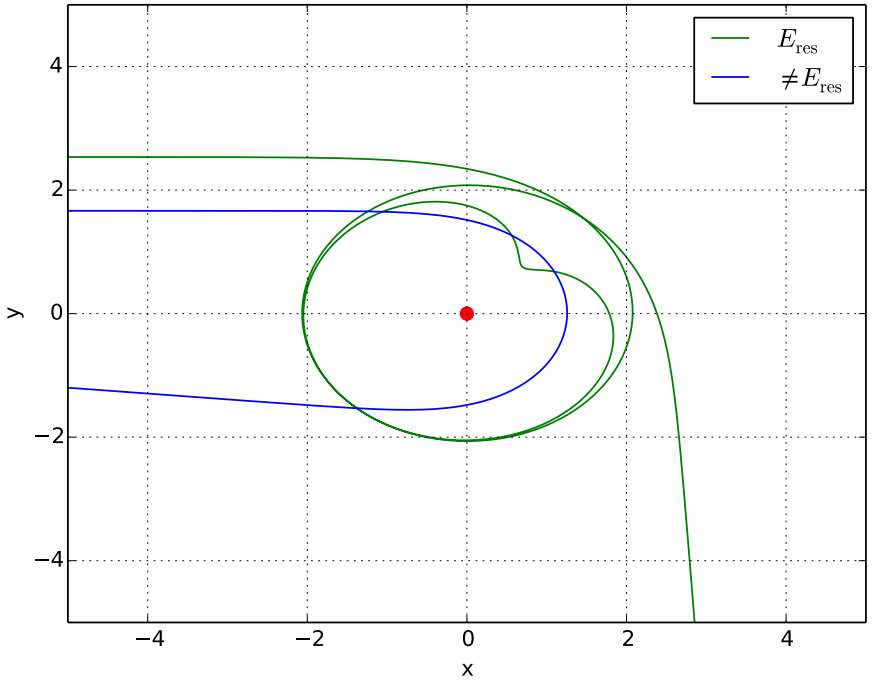

FIGURE 3.3: Classical scattering and difference between *resonant* orbits and other orbits – The example is two-dimensional and the red point represents one of the two atoms

However, in every possible interpretation, the important region that needs to be studied is where the potential presents a finite well, so let us define the following spatial integral that represents the radial probability to find the particle in the finite well at time t:

$$\rho(t) := \int_0^{2\sigma} dr' \, |u_l(r', t)|^2, \tag{3.26}$$

where $r_{\max} = 2\sigma$ is the position of the local maximum in the effective potential.
Then, the *permanence time* is defined as:

$$\mathcal{T} := \int_0^{\infty} dt' \rho(t'). \tag{3.27}$$

3.2.3 Imaginary potential

Parameters used to solve the time-dependent Schrödinger equation with the split-operator method are shown in Table 3.1.
The temporal evolution is stopped when the probability $\rho(t)$ is less than 10^{-4} and this happens when the wavefunction has almost left the finite well. Normally the duration of this time evolution is approximately $\Delta\bar{t} \simeq 1000$, but it clearly depends on the $\bar{k}$ value and other parameters of the initial wave packet.

As imaginary potential it has been chosen a parabolic function and Figure 3.2 gives an idea of the situation. The imaginary potential function is:

$$\mathrm{Im}[V(\bar{r})] = \begin{cases} -(a\bar{r}^2 + b\bar{r} + c), & 55 \leq \bar{r} < 80 \\ \\ 0 & 0 < \bar{r} < 55 \end{cases} \tag{3.28}$$

where a is chosen 0.0005, whereas b and c are fixed because the vertex of the parabola is at $\bar{r} = 55$.

Parameter	Value
Number N	4096
Reduced period $\bar{L}$	80
Step $\delta\bar{t}$	0.05
Starting position $\bar{r}_0$ of the wave packet	20
Sampling step $\delta\bar{r} = \bar{L}/N$	0.01953

TABLE 3.1: Parameters used with the split-operator method – For calculating the two integrals in (3.27), the trapezoidal rule has been used with precisions $\delta\bar{t}$ and $\delta\bar{r}$

Now it is necessary to prove the efficiency of this potential.
To do this, let us consider a Gaussian wave packet of the type (3.19) with $\bar{r}_0 = 20$, $\bar{\gamma} = 2.5$ and $\bar{k} > 0$. The *permanence time* $\mathcal{T}_{\text{refl}}$ defined in (3.27) is computed with a time evolution of $\Delta\bar{t} = 1000$. If the imaginary potential is efficient, the computed *permanence time* $\mathcal{T}_{\text{refl}}$ should be zero and there should not be spurious reflections of the wave packet. Results are shown in Table 3.2. In the range of interesting energies close to the resonance value (see Table 2.1), $\mathcal{T}_{\text{refl}} < 10^{-5}$ so the potential can be accepted. With other energy values, $\mathcal{T}_{\text{refl}}$ is no more negligible because there can be more spurious reflections or because the wave packet becomes wider very quickly. However, for the purposes of this thesis, the parabolic function can be definitely accepted.

$\bar{E}$	$\bar{k}$	$\bar{\mathcal{T}}_{\text{refl}}$
0.005	0.3770	0.6199
0.02	0.7541	0.008066
0.05	1.192	$9.287{\cdot}10^{-6}$
0.08145	1.522	$2.638{\cdot}10^{-6}$
0.2	2.385	$9.218{\cdot}10^{-8}$
0.9	5.059	$3.541{\cdot}10^{-6}$
2	7.541	0.0002254
8	15.08	0.01452

TABLE 3.2: Imaginary potential test with Gaussian wave packets with $\bar{\gamma} = 2.5$– The relation between $\bar{E}$ and $\bar{k}$ is $\bar{E} = \zeta\bar{k}^2$

3.2.4 A first qualitative description

Before analysing the problem in a quantitative way, in Figures 3.4, 3.5 and 3.6 it is shown the time-evolution of three different wave packets at three distinct instants. All three packets have $\bar{r}_0 = 20$ and a reduced width $\bar{\gamma} = 2.5$, whereas $\bar{k}$ is shown in the Figure's description.
As expected, only the wave packet in Figure 3.4 with an initial wave-vector $\bar{k}_{\text{res}}$ presents a wavefunction that is highly localized in the region with the finite well. This happens at $\bar{t} = 265$ and partially at $\bar{t} = 528$.

3.2.5 *Permanence time* as a function of k

The minimum width γ_{min} that satisfies the condition (3.24) is:

$$\bar{\gamma}_{\text{min}} = \sqrt{\frac{2\zeta}{\bar{\Gamma}}} = 2.504(6). \tag{3.29}$$

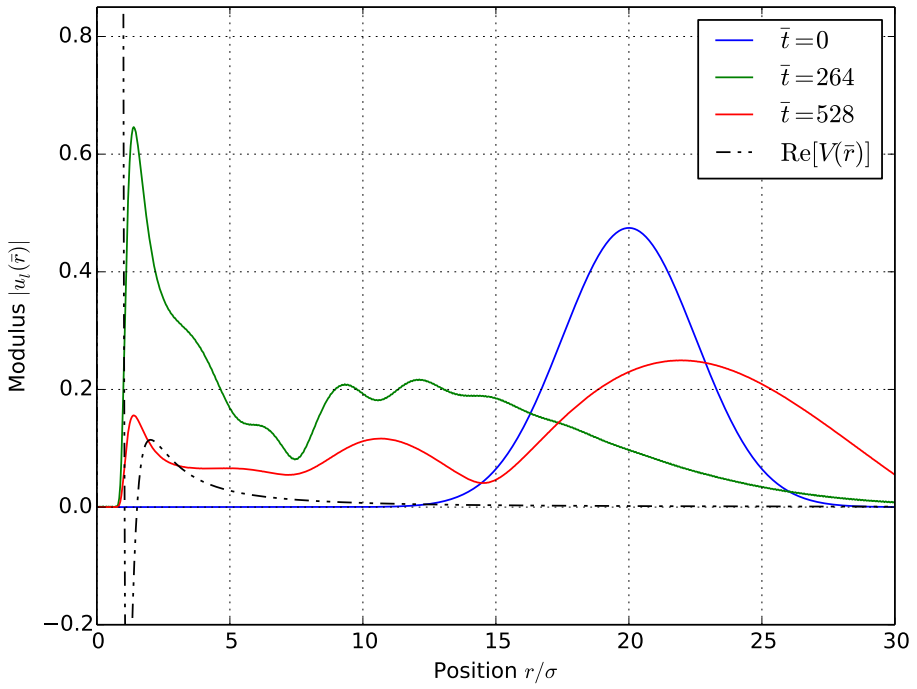

FIGURE 3.4: Time evolution of a *resonance* Gaussian wave packet with $\bar{k} = 1.5217$ $\bar{E} = 0.081446$

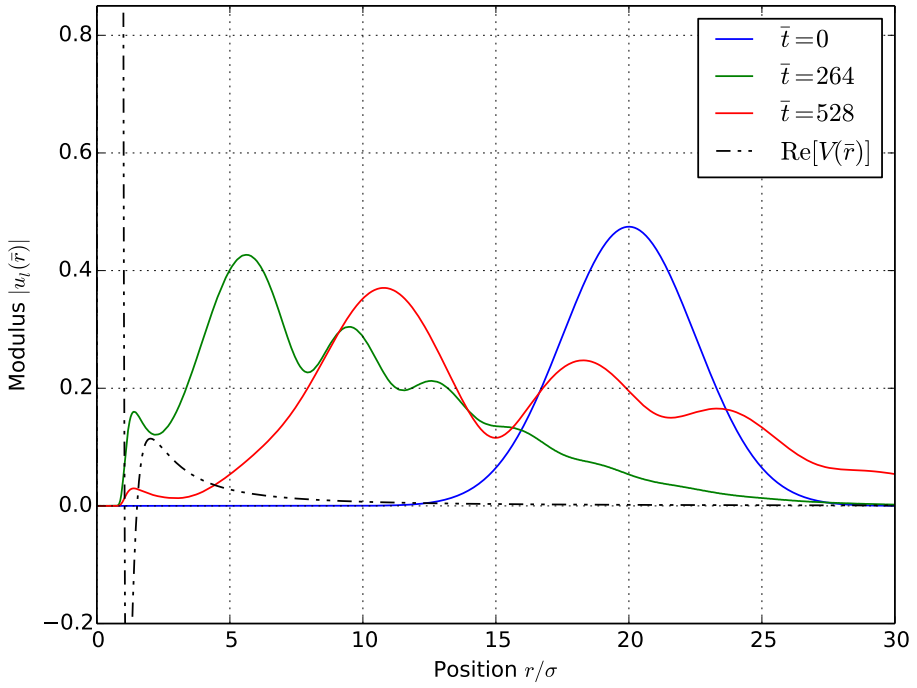

FIGURE 3.5: Time evolution of a Gaussian wave packet with $\bar{k} = 0.78087$ $\bar{E} = 0.021446$

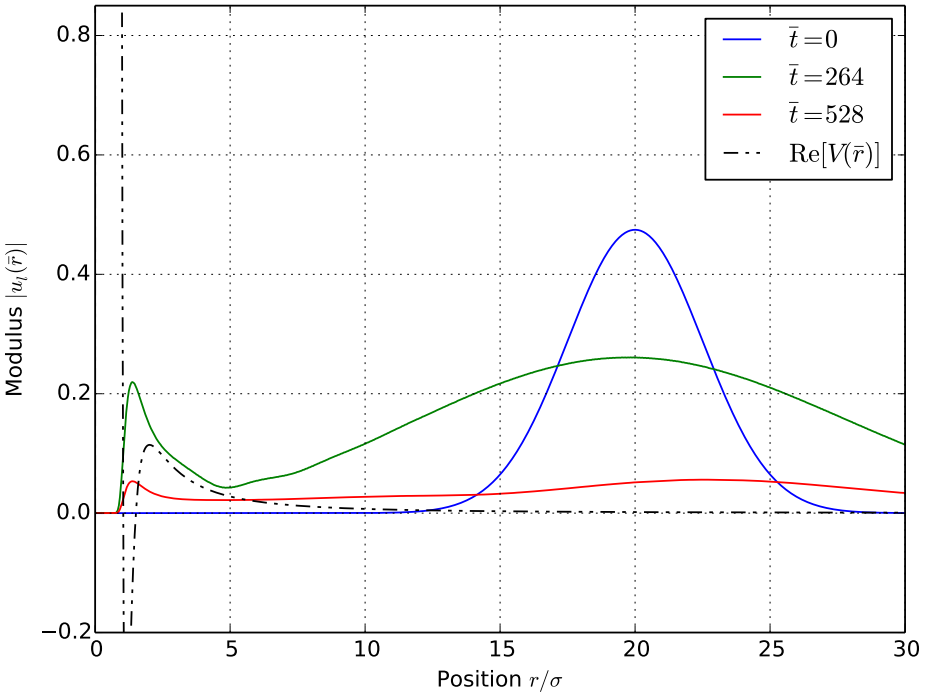

FIGURE 3.6: Time evolution of a Gaussian wave packet with $\bar{k} = 2.0887$ [$\bar{E} = 0.15344$]

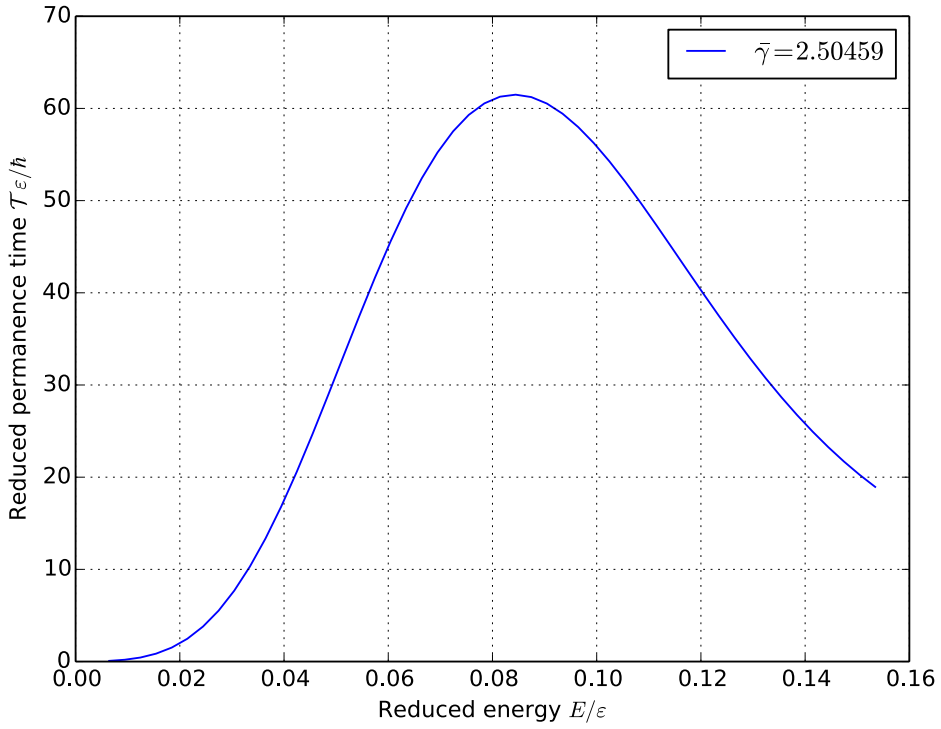

FIGURE 3.7: *Permanence time* as a function of energy in presence of a resonance

With a set of Gaussian wave packets that have $\gamma = \gamma_{\min}$ but different values of $\bar{k}$, the *permanence time* is expected to have a maximum when the $\bar{k}$ is close to $\bar{k}_{\text{res}}$ and Figure 3.7 confirms this assumption.
The blue line in Figure 3.8 shows a zoom of the previous plot in the region of the observed maximum, whose value is:

$$\bar{k}_{\max} = (1.548 \pm 0.001), \qquad \bar{E}_{\max} = (0.08431199 \pm 0.00000004), \tag{3.30}$$

and it is clearly larger than $\bar{E}_{\text{res}} = 0.081446$ (Table 2.1).
With a larger width $\bar{\gamma} = 3.5$ (green line in Figure 3.8) the value of this maximum becomes more similar to $\bar{E}_{\text{res}}$:

$$\bar{k}_{\max} = (1.535 \pm 0.001) \qquad \bar{E}_{\max} = (0.08283192 \pm 0.00000004). \tag{3.31}$$

The value $\bar{E}_{\text{res}}$ was found by solving the time-independent Schrödinger equation and in that case, in the region for large $\bar{r}$, the wavefunction has the form of a plane wave.
A Gaussian wave packet, in the limit $\gamma \to \infty$, becomes a plane wave of energy given by (3.22), so the value of the maximum is expected to tend exactly to $\bar{E}_{\text{res}}$ when $\gamma \to \infty$.

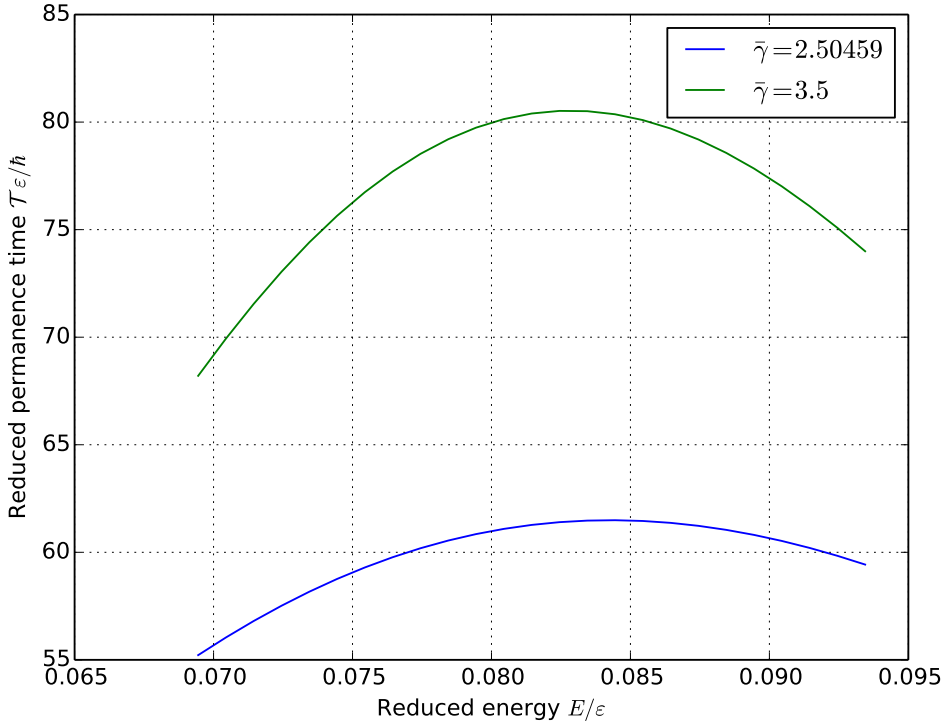

FIGURE 3.8: *Permanence time* as a function of energy with different widths

The green line in Figure 3.8 presents larger values of $\bar{\mathcal{T}}$, but this is consistent because with a larger value of γ the reciprocal wave packet has a smaller width and the plane wave components of the wave packet are more *resonant*.

3.2.6 *Permanence time* as a function of γ

Wave packets centered at the resonance – Let us consider a set of Gaussian wave packets with a fixed $\bar{k} = \bar{k}_{\text{res}}$ (see 3.22) and different values of $\bar{\gamma}$. The other parameters remain the same as in Table 3.1.
If $\bar{\gamma}$ increases, then the initial wave packet becomes larger and the reciprocal packet narrows, so there are fewer *not-resonant* components in the superposition and $\mathcal{T}$ is expected to rise. This is perfectly confirmed by the blue line in Figure 3.12.
In Figures 3.9, 3.10 and 3.11 it is shown how the quantity $\rho(\bar{t})$ in (3.26) evolves during the time evolution.
Gaussian wave packets that have small values of $\bar{\gamma}$, increase very quickly their width and it can be proved [Str14, pp. 25] that:

$$\bar{\gamma}(\bar{t}) = \sqrt{\bar{\gamma}^2 + \frac{\bar{t}^2\zeta^2}{\bar{\gamma}^2}}. \tag{3.32}$$

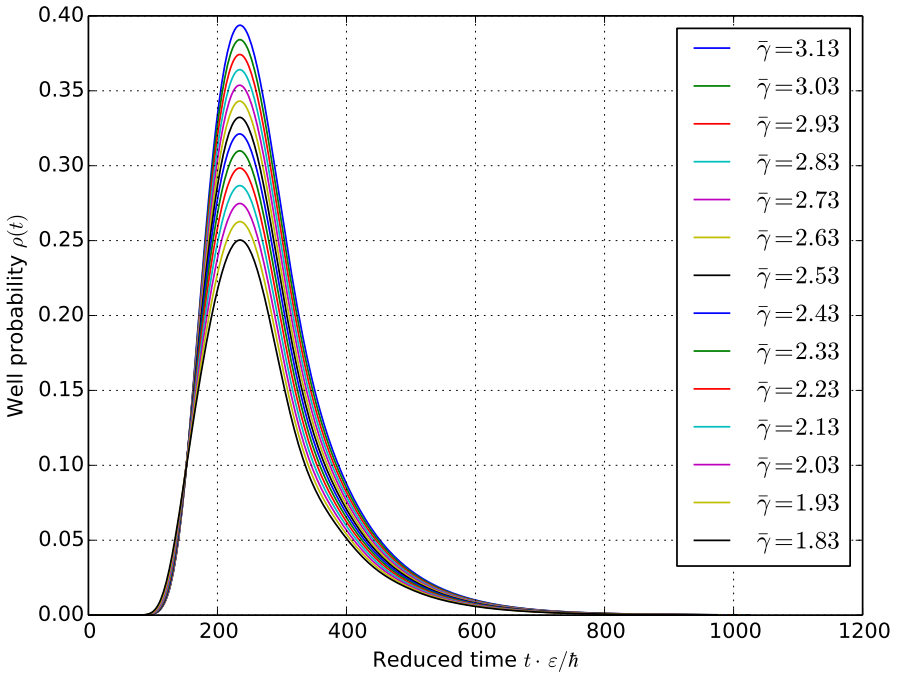

FIGURE 3.9: $\rho(\bar{t})$ and its time evolution for $\bar{k}_{\text{res}} = 1.522$

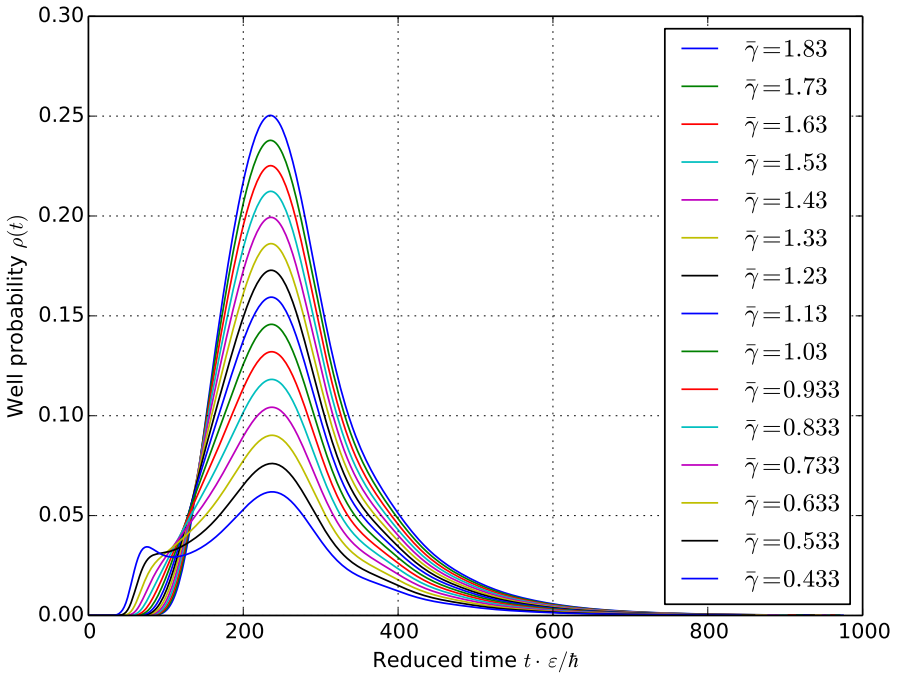

FIGURE 3.10: $\rho(\bar{t})$ and its time evolution for $\bar{k}_{\text{res}} = 1.522$

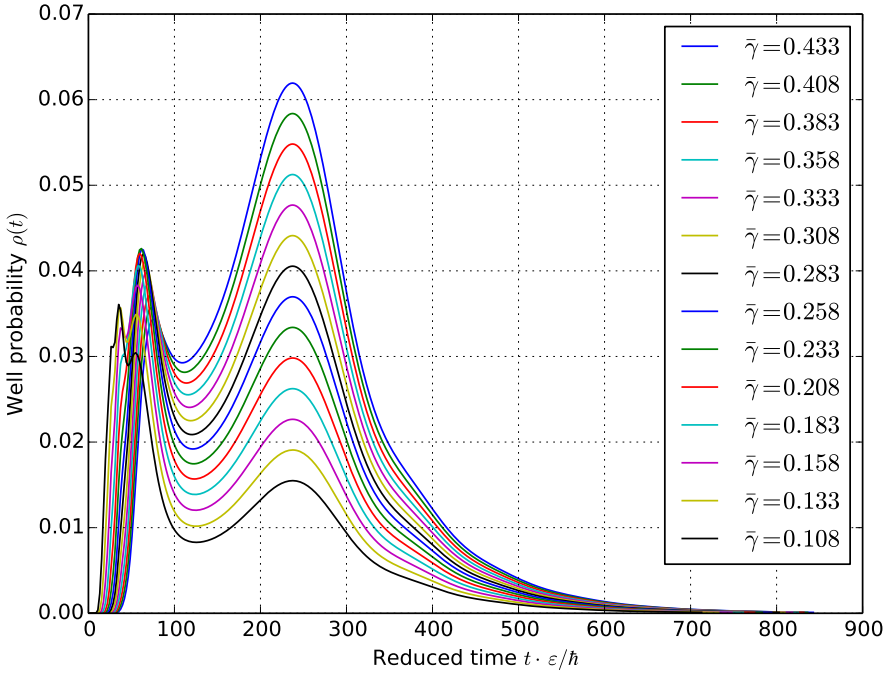

FIGURE 3.11: $\rho(\bar{t})$ and its time evolution for $\bar{k}_{\text{res}} = 1.522$

This explains what is shown in Figure 3.11 for small widths $\bar{\gamma}$. Indeed wave packets with small $\bar{\gamma}$ become wider very fast, so some parts of the wavefunction enter immediately in the finite well. But these are not *resonant* components because they have an energy too high, so great part of them are not able to pass through the finite barrier and are immediately reflected. It is only after a fixed amount of time that *resonant* components reach the barrier and the finite well.

Wave packets close to the resonance – In order to have a Gaussian wave packet that is not a good *resonant* wavefunction, the initial wave vector $\bar{k}$ has to satisfy:

$$\bar{k} \notin \left[\bar{k}_{\text{res}} - \frac{1}{\bar{\gamma}_{\text{min}}}, \bar{k}_{\text{res}} + \frac{1}{\bar{\gamma}_{\text{min}}} \right]. \tag{3.33}$$

The red and the green lines in Figure 3.12 represent two sets of these wave packets and as expected their values of *permanence time* are smaller than those of the *resonant* wave packets (blue line in Figure 3.12). In the last two cases the *permanence time* presents a maximum because if $\bar{\gamma}$ becomes smaller, the width of the reciprocal wave packet rises and the wavefunction becomes more *resonant*.
Then, if $\bar{\gamma} \ll \bar{\gamma}_{\text{min}}$, the *permanence time* $\bar{\mathcal{T}}$ does no longer depend from $\bar{k}$.

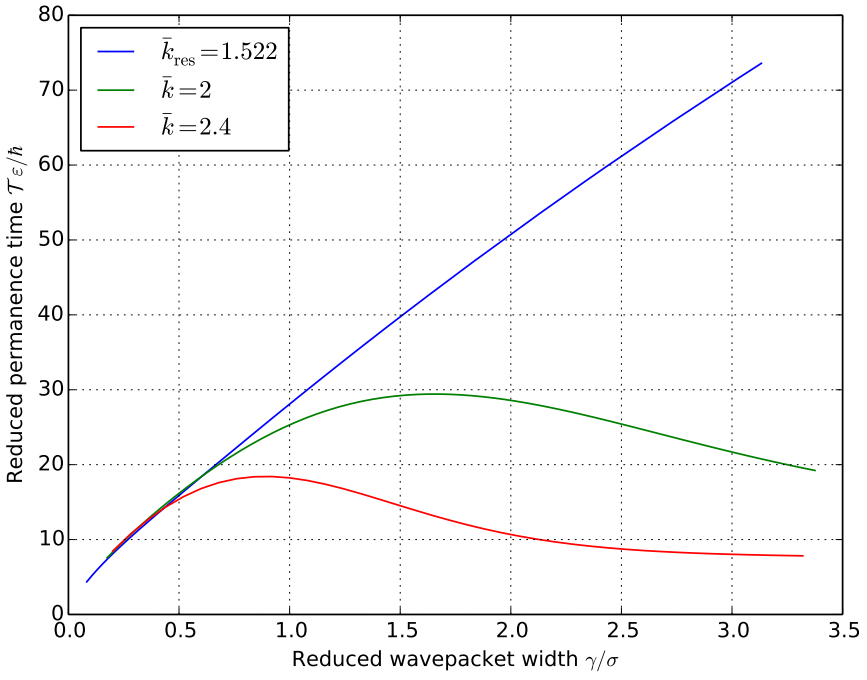

FIGURE 3.12: *Permanence time* as a function of width $\bar{\gamma}$ in three sets of wave packets with different initial $\bar{k}$

3.3 Metastable states

3.3.1 Bound states of the finite well

In a one-dimensional problem with a potential that presents a well with infinite barriers on its sides, the solutions of the time-independent Schrödinger equation are bound states with fixed energy values.
With the effective potential $V_{\text{eff}}(\bar{r})$ for $l = 4$ (Figure 2.12), there are bound states only for negative energies, however it is interesting to analyse how the bound states would be if the finite barrier on the right-hand was infinite.
In order to study this problem, the wavefunction is set to zero for $\bar{r} \geq \bar{r}_{\max}$, where $\bar{r}_{\max}$ represents the point where the potential becomes infinite and the wavefunction has a discontinuity in its derivative.
By limiting the system to this maximum point $\bar{r}_{\max}$, the Numerov algorithm can be used again to find the ground state. The energy of this state depends on the value of $\bar{r}_{\max}$: for a resonance energy $\bar{E}_{\text{res}} = 0.08144(6)$ it is necessary the following maximum point:

$$\bar{r}_{\max} = 4.108(2). \tag{3.34}$$

To find this number it has been used the Newton-Raphson algorithm. The parameters used with N-R and with Numerov are shown in Table 3.3, where the N-R precision is chosen 10^{-5} because $\bar{E}_{\text{res}}$ has a precision of five digits.

3.3.2 Time-evolution of the ground state

Now let us study the time-evolution of this *resonance* ground state. Parameters used with the split-operator integration are shown Table in 3.3.

Parameter	Value
Number N	8192
Reduced period $\bar{L}$	80
Time-step $\delta\bar{t}$	0.05
Sampling step $\delta\bar{r} = \bar{L}/N$	0.009766
Stop of the time-evolution	$\rho(\bar{t}) < 10^{-5}$
Numerov step h	$\delta\bar{r}$
Start point for Numerov $\bar{r}_{\min}$	0.7
Merge point for Numerov $\bar{r}_0$	1.3
Newton-Raphson precision	10^{-5}

TABLE 3.3: Parameters used with split-operator, Numerov and Newton-Raphson algorithms

	A	B	C	$\bar{\mathcal{T}}_{fit}$
$\varrho = 2$	1.189(8)	1.050(8)	1.349(3)	79.62(5)
$\varrho = 7$	1.594(7)	0.3585(3)	1.240(1)	82.30(6)

TABLE 3.4: Two fit of the ground state: results

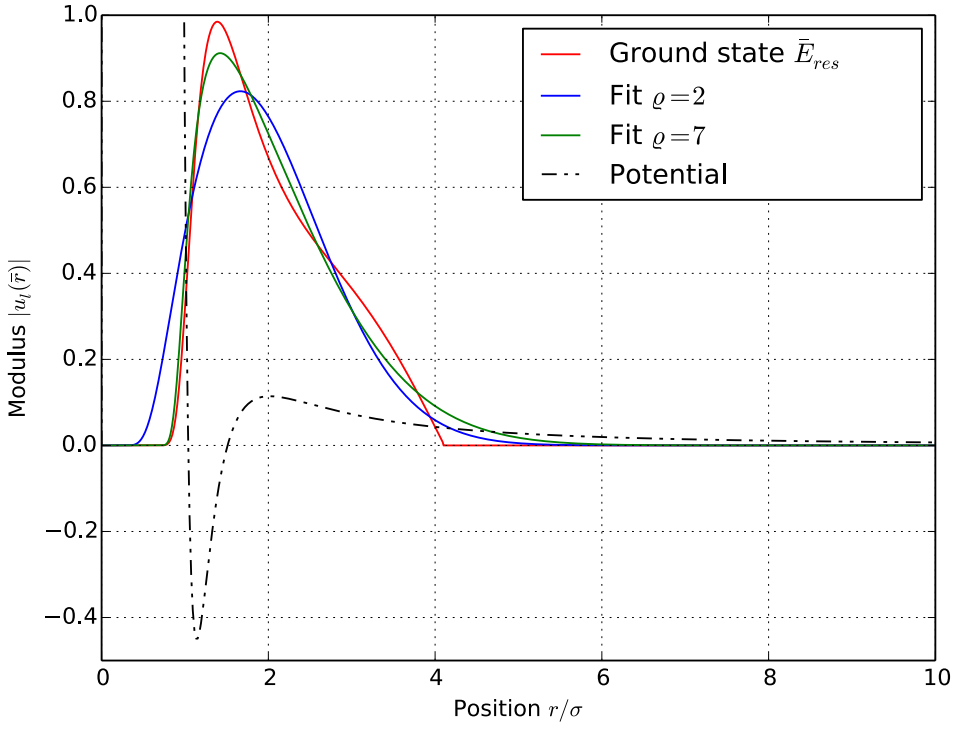

FIGURE 3.13: Comparison between the resonance ground state and the two fit

The *permanence time* (3.27) of this state is:

$$\bar{\mathcal{T}}_{\mathrm{GS}} = 84.05(5). \tag{3.35}$$

To prove that $\bar{\mathcal{T}}_{\mathrm{GS}}$ is one of the largest values of *permanence time*, let us fit this state with other similar functions and compare the values of $\bar{\mathcal{T}}$.
The problem with a Gaussian function is that it is too wide, so the tail of the wavefunction enters the infinite potential barrier for $\bar{r} \to 0$.
A possible alternative is the following function:

$$f_\varrho(\bar{r}) = C \cdot \exp\left[-\frac{(\bar{r} - A)^2}{2B^2} - \frac{1}{\bar{r}^\varrho}\right] \tag{3.36}$$

where A, B and C are parameters to fit. Unlike the Gaussian function, with the ϱ-term in the exponential, the wavefunction tends to zero faster for $\bar{r} \to 0$. Results for a fit with $\varrho = 2$ and another with $\varrho = 7$ are shown in Table 3.4 and Figure 3.13: as expected

$\bar{E}$	$\bar{r}_{\max}$	$\bar{\mathcal{T}}$
0.08144(6)	4.108(2)	84.05(5)
0.07835(2)	4.655(1)	78.53(3)
0.09145(3)	2.916(8)	77.27(9)

TABLE 3.5: Comparison between the resonance ground state (first line in the Table) and other two ground states with energies close to $\bar{E}_{\text{res}}$

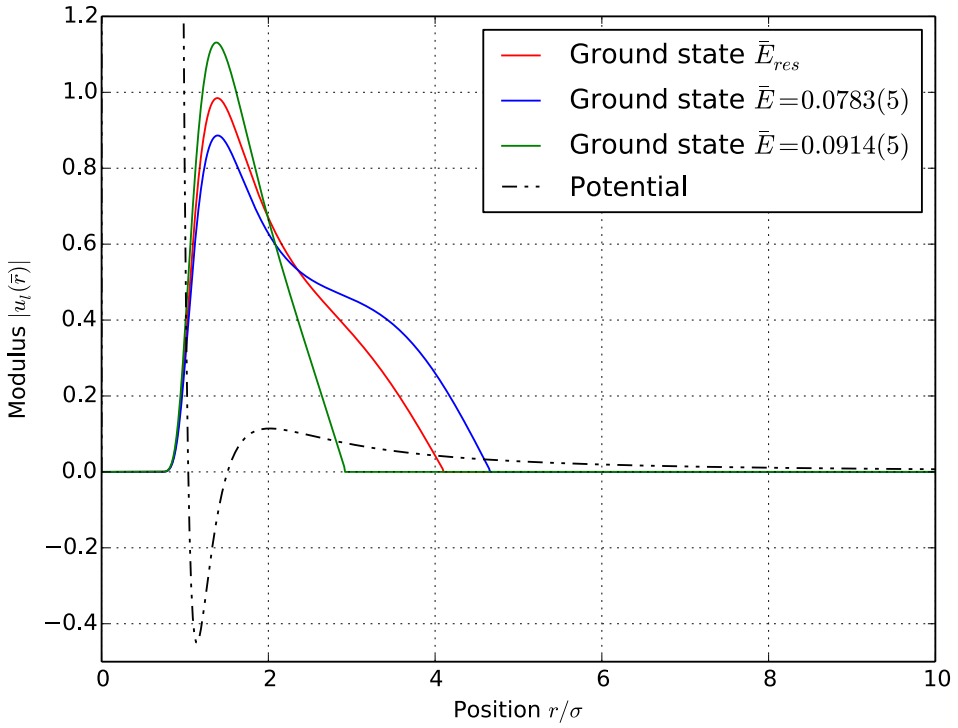

FIGURE 3.14: Comparison between three possible ground states with different energies

permanence time values are smaller than the one in (3.35).

Another possibility is to find other bound states with different $\bar{r}_{\max}$ and energies close to $\bar{E}_{\text{res}}$, but also in this case their *permanence time* is smaller than the resonance one (see Table 3.5).

An important remark – The three just mentioned different bound states of the Table 3.5 are shown in Figure 3.14, whereas their time-evolution at $\bar{t} = 16$ and $\bar{t} = 64$ can be seen respectively in Figures 3.15 and 3.16.
In the region of the finite well, the shape of the three states becomes approximately the same after the time-evolution, especially when $\bar{t} \gg 1$.
So it seems that every initial state tends to the same identical state after some time.

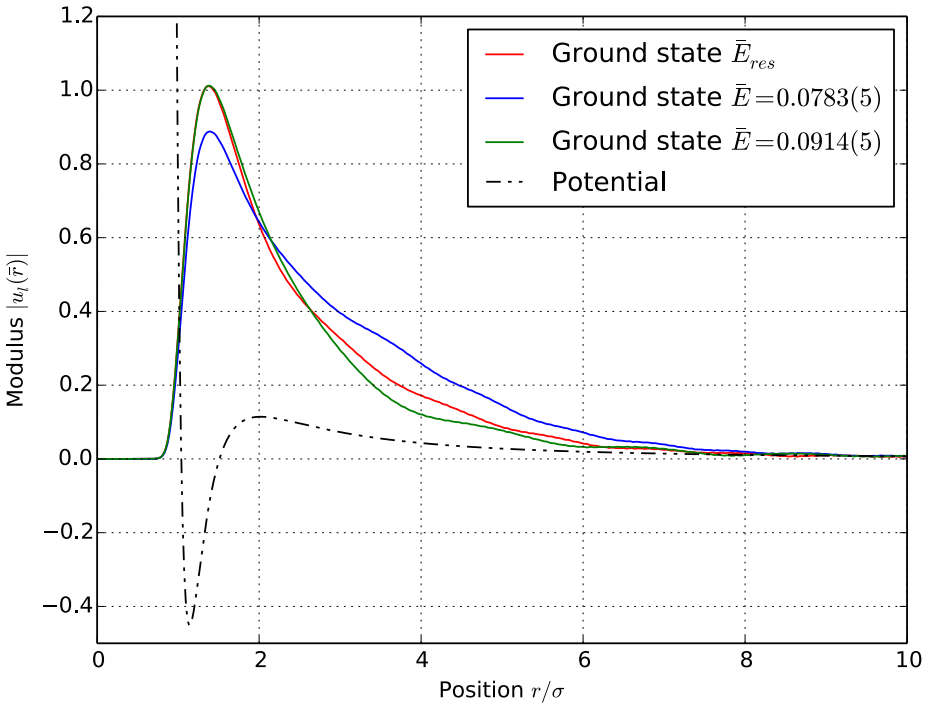

FIGURE 3.15: The same three states at time $\bar{t} = 16$

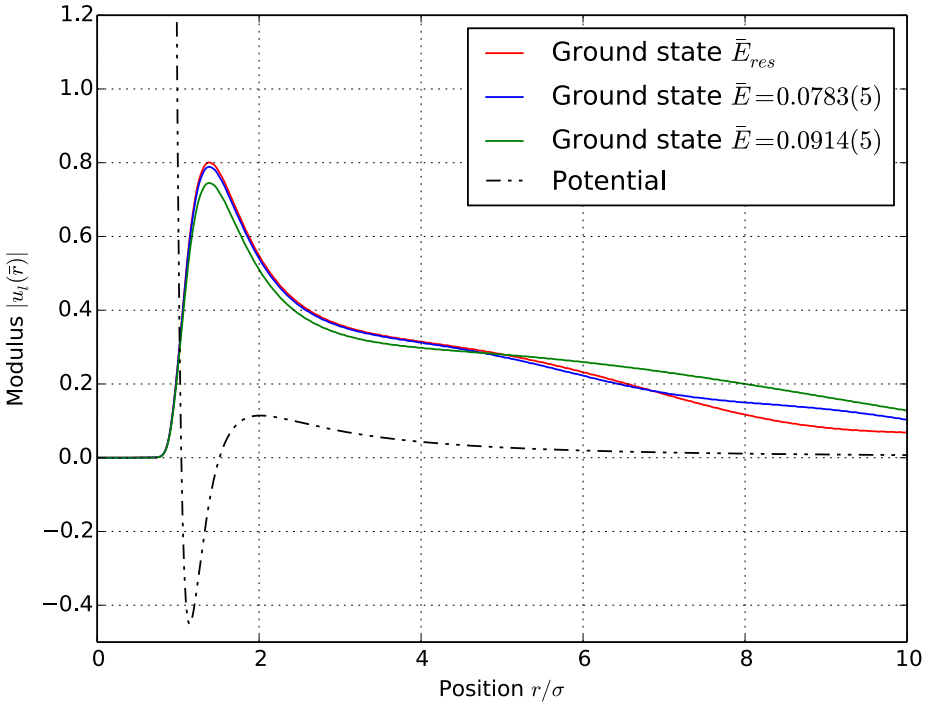

FIGURE 3.16: The same three states at time $\bar{t} = 64$

3.3.3 The *complex energies formalism* and the parameter Γ in the time-dependent problem

In a time-dependent approach, a system with the following complex energies

$$\tilde{E}_n = E_n - i\,\frac{\Gamma_n}{2}, \tag{3.37}$$

has a wavefunction that does not preserve the integral of the squared modulus:

$$\mathcal{P}(t) = \int_0^\infty dr\,|u_l(r,t)|^2 \neq \text{const.} \tag{3.38}$$

A decay state is initially localized in the finite well and then it slowly passes trough the finite barrier and leaves the well. By focusing only on the finite well and the range:

$$\bar{r} \in [0, \bar{r}_{\max}] \tag{3.39}$$

it is possible to justify the presence of a complex energy of the type (3.37) because in the finite well the state *vanishes* and the quantity:

$$\int_0^{\bar{r}_{\max}} d\bar{r}\;\sigma \cdot |u_l(\bar{r})|^2 \tag{3.40}$$

is no longer preserved.
Let us call $\phi_n(\bar{r})$ the solutions of the time-independent Schrödinger equation with this limited system. So every generic state ψ limited to the range (3.39) can be expanded in the complete basis set of these stationary wavefunctions:

$$\psi = \sum_n c_n \cdot \phi_n. \tag{3.41}$$

With complex energies the time evolution of every stationary state is given by:

$$|\phi_n(\bar{t})| = \exp\left(-\bar{t}\,\frac{\bar{\Gamma}_n}{2}\right)\,|\phi_n(0)| \tag{3.42}$$

and so it is possible to define also a reduced lifetime of the state as:

$$\bar{\tau} := \frac{2}{\bar{\Gamma}}. \tag{3.43}$$

Every state tends to the ground state – From the equation (3.42) it follows that:

$$\frac{|\phi_n(\bar{t})|}{|\phi_0(\bar{t})|} \propto \exp\left[-\bar{t}\left(\frac{\bar{\Gamma}_n - \bar{\Gamma}_0}{1}\right)\right]. \tag{3.44}$$

So the stationary states decay with different velocities, but the ground state is the one that decays more slowly if $\Gamma_n < \Gamma_{n+1}$. This condition can be shown in experiments [HG07, pp. 118–121], so let us assume it for the moment and see what are its consequences.
Then, the time evolution of a generic state ψ can be written:

$$\psi(\bar{t}) = \sum_n c_n \cdot \exp\left(-\bar{t}\,\frac{\Gamma_n}{2}\right) \cdot \exp\Big(-i\bar{t}\,\bar{E}_n\Big) \cdot \phi_n(0), \tag{3.45}$$

so when $\bar{t} \gg 1$ the first term of the sum predominates and the state ψ becomes approximately the ground state.

The parameter Γ – From equation (3.42) it follows that:

$$\left|\frac{\phi_0(\bar{t}_1)}{\phi_0(\bar{t}_2)}\right| = \exp\left[-\frac{\bar{\Gamma}_0}{2}\Big(\bar{t}_2 - \bar{t}_1\Big)\right], \tag{3.46}$$

that in terms of the parameter $\bar{\Gamma}_0$ is:

$$\bar{\Gamma}_0 = 2\frac{\ln\left[\left|\frac{\phi_0(\bar{t}_1)}{\phi_0(\bar{t}_2)}\right|\right]}{\bar{t}_2 - \bar{t}_1} \qquad \text{when} \quad \bar{t}_1, \bar{t}_2 \gg 1. \tag{3.47}$$

The resonance decay state shown in the first line of the Table 3.5 can be used to estimate this parameter. The point where to evaluate the wavefunction is chosen at $\tilde{r} = 1.5$ that is in the region of the finite well, whereas the chose time values are $\bar{t}_1 = 200$ and $\bar{t}_2 = 250$. The computed value of the parameter is:

$$\bar{\Gamma} = 0.01085(2). \tag{3.48}$$

It is comparable with the exact value of Table 2.1, so the assumption $\Gamma_n < \Gamma_{n+1}$ can be considered valid. The reason why the numbers in (3.48) and Table 2.1 are not exactly the same, can be that $\bar{t}_1$ and $\bar{t}_2$ are not enough large, so the relation (3.47) is not entirely valid.

Bibliography

[CT65] J. W. Cooley and J. W. Tukey. An algorithm for the machine calculation of complex Fourier series. *Math. Comput.*, (19):297–301, 1965. URL: http://www.ams.org/journals/mcom/1965-19-090/S0025-5718-1965-0178586-1/home.html.

[Gar14] G. Garberoglio. Computational Physics 1. Interdisciplinary Laboratory for Computational Science (LISC), Fondazione Bruno Kessler and University of Trento, 2014.

[Gau] Examples of the use of Schrödinger's equation. Study of a Gaussian Wave Packet. URL: http://www.colorado.edu/physics/phys2170/phys2170_sp07/downloads/Gaussian.pdf.

[HG07] E. M. Henley and A. Garcia. *Subatomic Physics*. World Scientific Publishing Co. Pte. Ltd., third edition, 2007.

[JPTW79] W. Welz J. P. Tonnies and G. Wolf. Molecular beam scattering studies of orbiting resonances and the determination of van der Waals potentials for H-Ne, Ar, Kr, and Xe and for H_2-Ar, Kr, and Xe. *J. Chem. Phys.*, (71):614, 1979. URL: http://scitation.aip.org/content/aip/journal/jcp/71/2/10.1063/1.438414.

[MDZ02] O. Schütze M. Dellnitz and Q. Zheng. Locating all the zeros of an analytic function in one complex variable. *Elsevier Science*, (138):325–333, 2002. URL: http://www2.math.uu.se/~warwick/vt09/FMB/FMB_reading/complexRoots/Dellnitz.pdf.

[Scr] C. Scrucca. Quantum Physics III. Swiss Federal Institute of Technology Lausanne, Instute for Theoretical Physics. URL: http://itp.epfl.ch/files/content/sites/itp/files/users/181759/public/qpIII.pdf.

[Str14] S. Stringari. Corso di Meccanica Quantistica I. University of Trento, 2014.